

N69-40383  
NASA GR 86258

2

# HETEROEPITAXY OF III-V COMPOUND SEMICONDUCTORS ON INSULATING SUBSTRATES

Interim Report

by Harold M. Manasevit and Arthur C. Thorsen

May 1969

## CASE FILE COPY

Distribution of this report is provided in the interest of information exchange. Responsibility for the contents resides in the author or organization that prepared it.

Prepared under Contract No. NAS 12-2010 by  
Physical Sciences Department of Autonetics,  
A Division of North American Rockwell Corporation, Anaheim, California

for

Electronics Research Center  
NATIONAL AERONAUTICS AND SPACE ADMINISTRATION

**HETEROEPITAXY OF III-V COMPOUND SEMICONDUCTORS ON INSULATING SUBSTRATES**

**Interim Report**

**by Harold M. Manasevit and Arthur C. Thorsen**

**May 1969**

Distribution of this report is provided in the interest of information exchange. Responsibility for the contents resides in the author or organization that prepared it.

Prepared under Contract No. NAS 12-2010 by  
Physical Sciences Department of Autonetics,  
A Division of North American Rockwell Corporation, Anaheim, California

for

Electronics Research Center  
NATIONAL AERONAUTICS AND SPACE ADMINISTRATION




## TABLE OF CONTENTS

	<u>Page</u>
SUMMARY .....	1
INTRODUCTION .....	2
EXPERIMENTAL STUDIES .....	3
Apparatus .....	3
Materials .....	5
Deposition Procedures .....	6
Evaluation Procedures .....	6
RESULTS AND DISCUSSION .....	8
Film Properties .....	8
Substrate Surface Properties .....	58
Reaction Mechanisms .....	59
CONCLUSIONS .....	60
REFERENCES .....	62
APPENDIX A, New Technology .....	63

## ILLUSTRATIONS

<u>Figure</u>		<u>Page</u>
1	Schematic of Deposition Apparatus . . . . .	4
2	Mobility vs Carrier Concentration for GaAs/ $Al_2O_3$ , Undoped Samples (Thickness Range: 4-30 $\mu$ m) . . . . .	19
3	Mobility vs Carrier Concentration for GaAs/ $Al_2O_3$ Undoped Samples (Thickness $\sim$ 10 $\mu$ m) — $H_2$ Process . . . . .	20
4	Mobility vs Carrier Concentration for GaAs/ $Al_2O_3$ Undoped Samples — Helium Process . . . . .	21
5	Variation of Carrier Concentration with Reciprocal Temperature for an Undoped GaAs/ $Al_2O_3$ Film . . . . .	24
6	Effect of Substrate Temperature on Rate of Growth of (111) GaAs on (0001) $Al_2O_3$ . . . . .	28
7	(110) RED Photographs of (111) GaAs/(0001) $Al_2O_3$ Films Grown at (a) 675C; (b) 800C; (c) 825C . . . . .	29
8	Replicas for (111) GaAs/(0001) $Al_2O_3$ Films Grown at Setting of 250-45-0 at 675C for (a) 1 Sec; (b) 3 Sec; (c) 5 Sec; (d) 7 Sec (All Replicas at 20,000X) . . . . .	30
9	Replicas and (110) RED Patterns for (111) GaAs/(0001) $Al_2O_3$ Films Grown at 675C at Setting of 200-45-0 for (a) 10 Sec; (b) 20 Sec; (c) 30 Sec. (All Replicas at 20,000X) . . . . .	31
10	(110) RED Patterns for (111) GaAs/(0001) $Al_2O_3$ Films Grown at 675C for 1 Sec, for Different $AsH_3$ Settings and Annealed at 675C for 1 Hr. . . . .	32
11	GaAs/(0001) $Al_2O_3$ Produced by Reaction of Residual TMG with $AsH_3$ for 1 Sec in an $AsH_3-H_2$ Atmosphere. a) Surface Structure at Magnification of 42,300X; b) (110) Reflection Electron Diffraction Pattern . . . . .	33
12	GaAs/(0001) $Al_2O_3$ Produced by Reaction of Residual TMG with $AsH_3$ for 6 Min in an $AsH_3-H_2$ Atmosphere. a) Surface Structure at Magnification of 42,300X; b) (110) Reflection Electron Diffraction Pattern . . . . .	34
13	Replicas for (111) GaAs/(0001) $Al_2O_3$ Films Grown at 675C for Different TMG Settings and Times. a) At 250-10-0 for 1 Sec; b) At 250-10-0 for 3 Sec; c) At 250-20-0 for 1 Sec; d) At 250-20-0 for 3 Sec. (All Replicas at 20,000X) . . . . .	36
14	Replicas for (111) GaAs/(0001) $Al_2O_3$ Films Grown for 1 Sec at Setting of 250-45-0. a) As Grown; b) After Annealing in $AsH_3$ for 1 Hr at 600C; c) After Annealing in $AsH_3$ for 1 Hr at 675C. (All Replicas at 20,000X) . . . . .	37
15	Replicas and RED Patterns for a GaAs/(0001) $Al_2O_3$ Film Grown for 3 Seconds at Setting of 250-45-0. (a) As Grown; (b) After Annealing in $AsH_3$ for 1 Hr at 600C; (c) After Annealing in $AsH_3$ for 1 Hr at 675C. (All Replicas at 20,000X) . . . . .	38

ILLUSTRATIONS (Cont)

<u>Figure</u>		<u>Page</u>
16	Replicas and RED Patterns for a GaAs/(0001) Al <sub>2</sub> O <sub>3</sub> Film Grown for 3 Seconds at Setting of 50-45-0. (a) As Grown; (b) After Annealing in AsH <sub>3</sub> for 1 Hr at 600C; (c) After Annealing in AsH <sub>3</sub> for 1 Hr at 675C (All Replicas at 20,000X)	39
17	Replicas and (110) RED Patterns for (111) GaAs/(0001) Al <sub>2</sub> O <sub>3</sub> Films Grown for 5 Seconds at Setting of 250-45-0. a) As Grown; b) After Annealing in AsH <sub>3</sub> for 1 Hr at 600C; c) After Annealing in AsH <sub>3</sub> for 1 Hr at 675C. (All Replicas at 20,000X)	40
18	Replicas for (111) GaAs/(0001) Al <sub>2</sub> O <sub>3</sub> Films Grown for 7 Sec at Setting of 250-45-0. a) As Grown; b) After Annealing in AsH <sub>3</sub> for 1 Hr at 600C; c) After Annealing in AsH <sub>3</sub> for 1 Hr at 675C. (All Replicas at 20,000X)	41
19	Replicas and (110) RED Patterns for (111) GaAs/(0001) Al <sub>2</sub> O <sub>3</sub> Films Grown for 10 Sec at Setting of 250-45-0. a) As Grown; b) After Annealing in AsH <sub>3</sub> for 1 Hr at 600C; c) After Annealing in AsH <sub>3</sub> for 1 Hr at 675C; d) After Annealing in AsH <sub>3</sub> for 1 Hr at 725C (All Replicas at 20,000X)	42
20	Replicas for (110) RED Patterns for (111) GaAs/(0001) Al <sub>2</sub> O <sub>3</sub> Films Grown for 30 Sec at Setting of 250-45-0. a) As Grown; b) After Annealing in AsH <sub>3</sub> for 1 Hr at 675C; c) After Annealing in AsH <sub>3</sub> for 1 Hr at 725 C. (All Replicas at 20,000X)	43
21	Effect of Annealing on the Mobility of Three GaAs/Al <sub>2</sub> O <sub>3</sub> Films	45
22	The Effect of Grain Boundaries in the Verneuil Spinel on the Growth of GaAs	47
23	A Lang X-ray Topograph of (100) Czochralski Spinel Revealing Strained Areas (Dark Portions) in the Crystal (about 0.5 in. square)	47
24	Reflectivity of (100) GaAs Growth on a 0.5-Inch Wide (100) Spinel Substrate	48
25	Surface Structure of (100) GaAs Growth on (100) Spinel	49
26	Hole Concentration in (111) GaAs Films Grown on (0001) Al <sub>2</sub> O <sub>3</sub> as a Function of Diethylzinc (DEZ) and Trimethylgallium (TMG) Concentration	50
27	Portion of a Stereographic Projection of Al <sub>2</sub> O <sub>3</sub> . The symbol  Indicates Orientations Investigated.	52
28	(0001) Al <sub>2</sub> O <sub>3</sub> (a) with GaAs Film; (b) without Film, as Seen Between Crossed Polaroids	57

## TABLES

<u>Table</u>	<u>Page</u>
I. Electrical Properties of Epitaxial (111) GaAs/(0001) Al <sub>2</sub> O <sub>3</sub> as a Function of AsH <sub>3</sub> Concentration and Film Thickness at 650-660C . . . . .	9
II. Electrical Properties of Epitaxial (111) GaAs/(0001) Al <sub>2</sub> O <sub>3</sub> as a Function of TMG Concentration and Film Thickness at 650-660C . . . . .	10
III. Electrical Properties of Epitaxial (111) GaAs/(0001) Al <sub>2</sub> O <sub>3</sub> as a Function of AsH <sub>3</sub> and TMG Concentration at 675 C . . . . .	11
IV. Electrical Properties of Epitaxial (111) GaAs/(0001) Al <sub>2</sub> O <sub>3</sub> as a Function of TMG and AsH <sub>3</sub> Concentrations at 700 C . . . . .	12
V. Electrical Properties of Epitaxial (111) GaAs/(0001) Al <sub>2</sub> O <sub>3</sub> Grown Using H <sub>2</sub> as Carrier Gas and Ten Percent AsH <sub>3</sub> in H <sub>2</sub> . . . . .	14
VI. Electrical Properties of Epitaxial (111) GaAs/(0001) Al <sub>2</sub> O <sub>3</sub> Grown at 700 C and Constant AsH <sub>3</sub> Conditions, Using Five-9s He as Carrier Gas and Ten Percent AsH <sub>3</sub> in H <sub>2</sub> . . . . .	15
VII. Electrical Properties of Epitaxial (111) GaAs/(0001) Al <sub>2</sub> O <sub>3</sub> Grown at 700 C and Constant TMG, Using Five-9s He as Carrier Gas and Ten Percent AsH <sub>3</sub> in He . . . . .	16
VIII. Electrical Properties of Epitaxial (111) GaAs/(0001) Al <sub>2</sub> O <sub>3</sub> Grown Under Different Conditions, Using Six-9s He as Carrier Gas and Ten Percent AsH <sub>3</sub> in He . . . . .	17
IX. Electrical Properties of Epitaxial (111) GaAs/(0001) Al <sub>2</sub> O <sub>3</sub> as a Function of Layer Thickness for a Given AsH <sub>3</sub> -TMG Ratio (250-35-0)* at 675 C . . . . .	23
X. Study of the Formation and Effect of the Gray Stage at 675 C in an H <sub>2</sub> Atmosphere . . . . .	25
XI. GaAs/Al <sub>2</sub> O <sub>3</sub> Crystallographic Relationships From X-ray Diffraction Studies . . . . .	53

# HETEROEPITAXY OF III-V COMPOUND SEMICONDUCTORS ON INSULATING SUBSTRATES

By H. M. Manasevit and A. C. Thorsen

Autonetics Division of North American Rockwell Corporation  
Anaheim, California

## SUMMARY

Thick ( $>15\mu\text{m}$ ) undoped GaAs films with room temperature mobilities between 5000 and  $6000\text{ cm}^2/\text{V}\text{-sec}$  for carrier concentrations in the range from  $\sim 10^{16}$  to  $\sim 10^{17}\text{ cm}^{-3}$  have been grown on (0001)  $\text{Al}_2\text{O}_3$  by the trimethylgallium (TMG)-arsine ( $\text{AsH}_3$ ) process over the temperature range 650-700C.

The carrier concentrations of the resulting films are found to depend primarily on the purity of the starting materials and carrier gases used in growing the films. Depending on the source of  $\text{AsH}_3$  and TMG, net impurity concentrations in the films may range from  $\sim 10^{15}$  to over  $10^{17}\text{ cm}^{-3}$ . It has also been demonstrated that good quality films can be obtained by using either  $\text{H}_2$  or He as a carrier gas.

The quality of the films was also shown to be quite dependent on the relative  $\text{AsH}_3$ -TMG concentrations. By manipulation of this ratio it is possible to control to some extent the carrier concentration, resistivity, and even conductivity type of the resultant films.

The first few microns of growth of an intentionally undoped GaAs film have in general been shown to be p-type. With subsequent growth, the sample reverts to n-type with a continuing improvement in film quality. The average mobilities of  $\sim 5000\text{ cm}^2/\text{V}\text{-sec}$  measured in thick films can therefore be considered quite reasonable for such a graded structure.

Nucleation studies of the growth of very thin (i. e. ,  $\leq 1\mu\text{m}$ ) films of GaAs have shown that the early stages of growth appear to involve formation of small islands with pyramidal structure. A smoothing of the surface evidently occurs shortly after complete coverage is obtained. Reflection electron diffraction studies indicate some improvement in the crystal structure in thin layers with heat treatment, and corresponding electrical measurements on heat-treated samples show a trend toward a reduction in the net acceptor concentration.

GaAs/ $\text{Al}_2\text{O}_3$  orientation relationships have been extensively investigated. The studies to date, which encompass several orientations on six major crystallographic zones in  $\text{Al}_2\text{O}_3$ , reveal a preference for (111) GaAs growth, with pronounced twinning being the rule rather than the exception. The (0001)  $\text{Al}_2\text{O}_3$  plane has been the best plane for deposition; twin-free deposits of GaAs have been grown on this orientation.

Doping studies using diethylzinc (DEZ) as the p-type dopant have indicated that the final hole concentration is dependent on the growth rate and temperature as well as on the concentration of DEZ.



Preliminary low-energy electron diffraction (LEED) studies suggest that the (0001)  $Al_2O_3$  surface is not strongly affected by cleaning treatments with the "usual" solvents prior to GaAs film growth. However, sample exposure to different ambient conditions before LEED observations seriously affects the results. Therefore, a more complete study of the effect of environmental conditions on surface structure and chemistry may be necessary.

Electrical measurements made on homoepitaxial films of GaAs on Cr-doped GaAs indicate higher mobilities in thin films ( $\sim 3.5\mu m$ ) than are obtained for heteroepitaxial growth but essentially equivalent quality in thick films ( $\sim 48\mu m$ ). The limitations in mobility seem to be dependent specifically on the purity of the starting materials.

## INTRODUCTION

Some of the highest purity Ga-V compounds prepared today are made by epitaxial growth on GaAs employing chemical vapor deposition (CVD) techniques (Ref. 1, 2). Therefore, most of the various reported CVD methods were initially tested in our laboratories to attempt the growth of GaAs on insulating substrates.

In the early stages of the investigation, the  $HCl$ -transport open-tube process was used. Using a geometry involving close-spacing between the substrate and a polycrystalline GaAs source, epitaxial films of GaAs were achieved on GaAs and/or Ge, but no continuous-film growth was formed on  $Al_2O_3$ . When growth did occur, it was traced to the presence of Ge (Ref. 3) used as a companion substrate for simultaneous deposition in the same experiment.

Failure to achieve epitaxial growth of GaAs directly on insulating substrates by the  $HCl$  transport method without the intermediate Ge nucleating film was at first attributed only to the presence of  $HCl$  in the environment in concentrations greater than that necessary for it to function as a transport agent. A few attempts were made in the close-space system to control the  $HCl$  concentration by using  $AsCl_3$  as the transport agent, but the results were not encouraging.

The results suggested that the process used for promoting growth on insulators should be free from halides and any other transport agents that might contact and change the insulator surface in some way. However, the then-existing CVD processes all relied upon such transporting agents; so a new method for compound-semiconductor formation was desired.

A process for epitaxial film growth was sought which would have at least the following attributes:

1. Low temperature film growth, to minimize decomposition of the resultant film.
2. Formation of the compound at the heated substrate.
3. A single temperature zone, for simplicity in film formation and apparatus.

4. No gaseous etchants, to minimize possible substrate surface problems and remove complications due to autodoping.
5. Compatibility with gas-phase dopants, for in situ doping during film formation.

These attributes were realized when Autonetics demonstrated (Ref. 4) that Ga-Group V semiconductor films could be produced on GaAs, Ge, and insulating substrates by decomposing organo-gallium compounds and Group V hydrides. This deposition process appeared to offer the best means for achieving epitaxial films with reproducible properties. Although the growth of single-crystal films of GaAs on  $Al_2O_3$  and other substrates had been demonstrated (Refs. 4, 5), optimization of the process to produce films with properties approximating those of bulk material was necessary. A thorough variable-parameter study was indicated.

This report summarizes such work, accomplished under NASA Contract No. NAS 12-2010 during the period July 1, 1968 - March 31, 1969.

## EXPERIMENTAL STUDIES

Work on the contract program was begun early in July 1968. The company-supported effort carried out prior to that time provided a good base for pursuit of the proposed contract program. The principal activities from July 1, 1968, to March 31, 1969, were in the following important areas: deposition parameters, materials purity, crystal perfection, doping, orientation relationships, and nucleation studies.

### Apparatus

The apparatus presently in use consists principally of a vertical 60-mm-O. D. quartz tube 38 cm long, containing a SiC-covered C pedestal which can be inductively heated; stainless-steel bubblers containing the liquid organo-metallic compounds; appropriate flowmeters for monitoring the carrier gas,  $AsH_3$ , and dopant gas flows; a  $H_2$  burn-off area; and a manifold made from 1/4-in. stainless-steel tubing. Provisions are made for bypassing the quartz reactor and keeping the reactants separate until the gases are equilibrated and ready to be mixed for film formation. A schematic of the apparatus is shown in Figure 1.

During the course of the study several modifications have been made in the reactor portion of the system in order to assure a more uniform temperature control of the SiC-covered pedestal. By modifying the induction coil and minimizing the physical contact between the pedestal and the support rod, temperatures could be regulated to  $\pm 5$  deg C from the center of the 1.5-in.-diameter pedestal to within 1/4 in. of the pedestal edge. Provision has also been made to provide rotation of the pedestal during the deposition process. Film thickness control within 10 percent across a 1 1/2 in.-diameter pedestal is being achieved routinely.

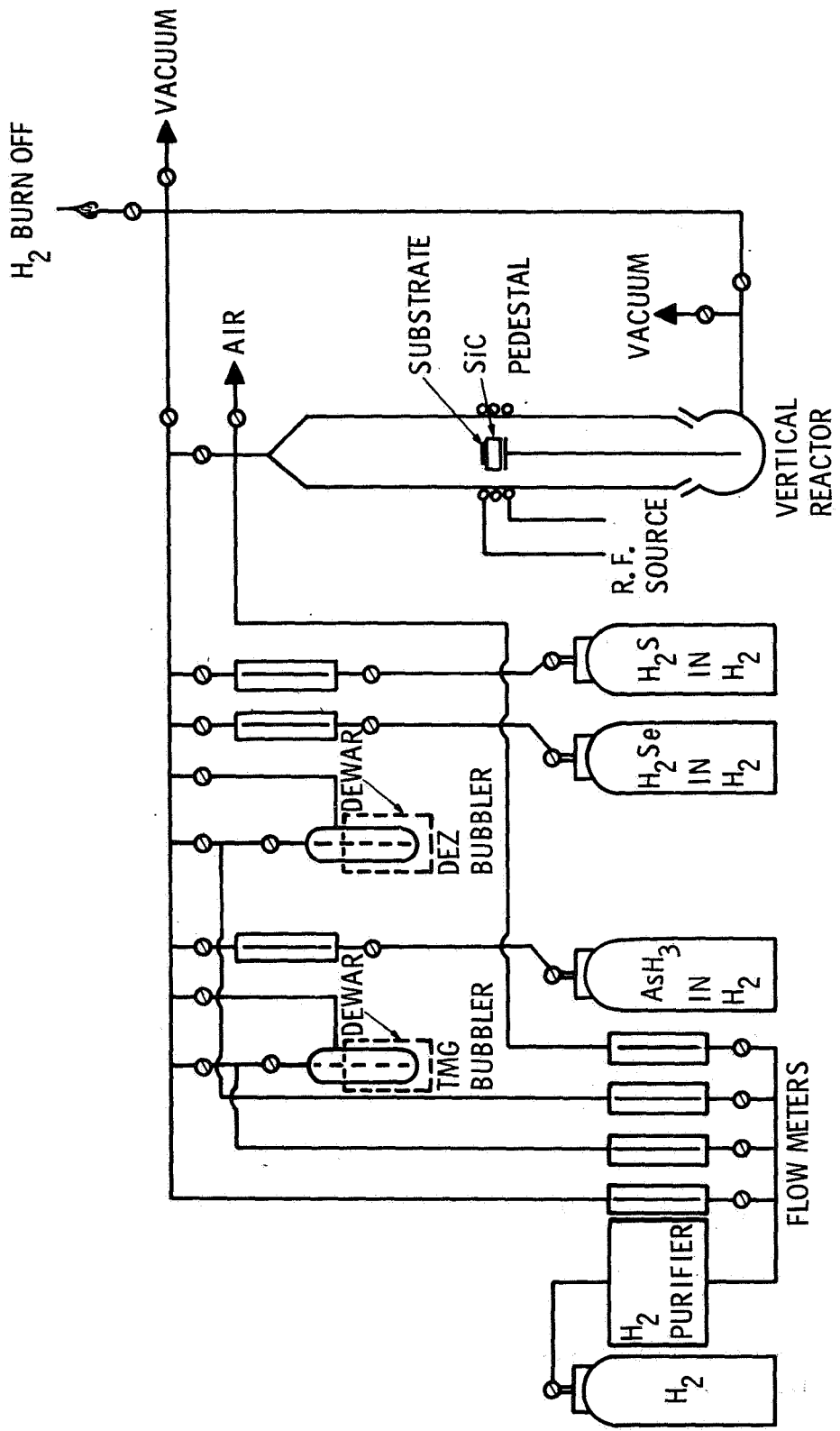


Figure 1. Schematic of Deposition Apparatus

Temperatures reported are those of the SiC-coated pedestal, as measured with an infrared radiation thermometer through the quartz reactor tube. The readings of the thermometer were compared with those of an optical pyrometer for pedestal temperatures greater than 750C. This provided a means for establishing an average emissivity value for the system in this temperature range. With this value the infrared thermometer signal readings were then extrapolated to still lower temperatures. All "deposition temperatures" reported here have been measured in this way.

## Materials

Arsine (AsH<sub>3</sub>). -- The AsH<sub>3</sub> in use to date during these studies has been obtained from three different suppliers. It has been found necessary to use in-stream purification of the AsH<sub>3</sub>, nominally 10 percent in H<sub>2</sub> or He, to remove major impurities which probably are residuals from the process used to clean the cylinders prior to filling with the gas mixtures. AsH<sub>3</sub>-and-gas mixtures from a fourth supplier will soon be delivered for evaluation. In-house studies using pure AsH<sub>3</sub> are to begin in the near future in an attempt to alleviate the impurity problem. The suppliers of the AsH<sub>3</sub>-and-gas mixtures are also attempting to correct this problem.

Trimethylgallium (TMG). -- The TMG has been obtained from several commercial sources but made to order in each case for our specific investigations. The study has included TMG made from three-9s Ga, four-9s Ga, four-9s Ga halide, and six-9s Ga halide. The material made from three-9s Ga was obtained in an "unpurified" state and subsequently purified in our laboratory after evaluation in the "unpurified" form. The TMG made from four-9s Ga and from Ga halide was purchased already prepurified by the vendor. These materials were used initially as received, by transferring the liquid directly into the bubbler, freezing and pumping on the TMG while it was under vacuum, admitting an atmosphere of the carrier gas, and equilibrating at 0C. The TMG was carried into the reactor for film growth by a carrier gas of H<sub>2</sub> or He passing through the liquid. The appearance of the grown layer indicated whether or not the TMG was adequate for growth studies.

Dopants. -- Both n- and p-type dopant impurities have been introduced into the GaAs layers in these investigations.

N-type. -- Both H<sub>2</sub>Se in H<sub>2</sub> and H<sub>2</sub>S in H<sub>2</sub> had been evaluated prior to this contract as to their compatibility with the metal-organic system and as dopants for the GaAs films being grown. The nominal tank concentrations were 500 and 200 ppm, respectively, in the carrier gas. However, these mixtures also required in-line purification to remove residual impurities, which were found to be reactive with the TMG.

P-type. -- Diethylzinc (DEZ) has been used as the p-type dopant for the GaAs films. The DEZ is normally purged with the carrier gas at -23C for about 30 minutes in order to remove the more volatile impurities, and then stored at 0C under the carrier gas until used for doping experiments. During doping, the "bubbling" tube is kept above the liquid surface. Carrier gases doped with diethylzinc are presently on order.

Carrier gases. -- Both H<sub>2</sub> and He have been used successfully as carrier gases in preparing GaAs from TMG and AsH<sub>3</sub>. It was observed in the studies with He that if purified "Grade 4.5<sup>TM</sup>" is used as the carrier gas, then special repurification of the TMG was occasionally necessary and beneficial in order to provide high quality reflective films. Such handling was not required when "Grade 6<sup>TM</sup>" He or Pd-purified H<sub>2</sub> was used. However, "Grade 4.5<sup>TM</sup>" He was often adequate if the He was passed through a liquid-N<sub>2</sub> trap placed near the gas source. A condensate, presumably H<sub>2</sub>O, was obtained. A condensate was also obtained at -196C from "Grade 6<sup>TM</sup>" He, and standard practice in our laboratories now involves this purification step for He. The major advantage of using the six-9s material with a -196C in-line purification lies presumably in the lower hydrocarbon and O<sub>2</sub> impurity levels, as compared with the levels reported in "Grade 4.5<sup>TM</sup>."

Substrates. -- Most of the Al<sub>2</sub>O<sub>3</sub> and spinel substrates used in these investigations have been polished commercially by vendors specializing in such work. Although the standard specification to the vendor requires "no polishing scratches visible at 400X," it has generally been difficult to obtain consistently good polished surfaces on the Al<sub>2</sub>O<sub>3</sub> substrates. The ease of obtaining a good polish is dependent upon the crystallographic orientation of the surface; some orientations are sensitive to the differences in the polishing procedures used by various vendors (these same observations held true when substrates were being obtained for the Si-on-Al<sub>2</sub>O<sub>3</sub> investigations). In some instances, substrates polished by one vendor had to be repolished by another before GaAs epitaxy could be successfully achieved on the Al<sub>2</sub>O<sub>3</sub> surfaces. GaAs epitaxy is found to be much more sensitive to the Al<sub>2</sub>O<sub>3</sub> substrate surface conditions than is Si epitaxy.

Since the Al<sub>2</sub>O<sub>3</sub> polishing procedures of the vendors are generally proprietary, it was determined that the necessary polishing methods for Al<sub>2</sub>O<sub>3</sub> (and other insulating substrate materials) should be developed at Autonetics in the Semiconductor Materials Group. Considerable progress has been made toward this end, and (0001) Al<sub>2</sub>O<sub>3</sub> substrates final-polished in-house have been found to be superior to those prepared by outside sources.

### Deposition Procedures

The deposition procedures now in effect involve the growth of GaAs films in an atmosphere of As produced by decomposing AsH<sub>3</sub> at the hot pedestal for two or three minutes prior to the introduction of the TMG into the reactor. When the substrate is GaAs, an As atmosphere is formed from AsH<sub>3</sub> at about 600C in order to prevent decomposition of the substrate at the higher growth temperature. AsH<sub>3</sub> flow is also continued after the deposition is completed until the temperature has dropped to about 600C.

Dopant gases are normally added to the TMG gas stream but are also found to be compatible with the AsH<sub>3</sub>.

### Evaluation Procedures

Much of the effort of this program has been directed to evaluating the characteristics of the GaAs layers by a variety of metallurgical, optical, and electrical techniques.

Metallurgical. -- Following deposition, the epitaxial layers are routinely examined by optical microscopy. It is usually possible to identify good epitaxy by visual inspection. Beyond inspection of the epitaxial layers by optical microscopy, extensive investigation of the thickness, surface characteristics, and crystallographic perfection of the deposited semiconductor is carried out. The film thicknesses are measured by observation of the interference fringe pattern in the reflectance spectrum in the infrared region, as obtained with a Beckman IR-5A double-beam spectrophotometer, or by a tracing made with a Talysurf surface-roughness gauge with stripchart recorder.

Considerable knowledge of the nature of the epitaxial films has been gained by x-ray diffraction techniques. These are being used for evaluating both the substrate defect structure and that of the deposited overgrowth. Laue back-reflection x-ray patterns are used to select composites for full-circle goniometer determination of the orientation relationships and twin structures.

Lang-type topography cameras are used to provide highly informative displays of the defect structure throughout the crystal being examined. This technique has been applied to several of the substrates used in this program. Replica electron microscopy and reflection electron diffraction (RED) are used as required to screen the epitaxial composites prior to x-ray evaluation, to examine the substrate and surface of the GaAs deposit for inhomogeneities, and to reveal changes which occur during the nucleation and annealing studies.

Electrical. -- The measurement of the fundamental electrical properties to characterize the semiconductor films prepared in this program has constituted an extremely valuable part of the investigations. The electrical measurements may range from routine determination of conductivity type with a thermoelectric probe to detailed studies of carrier-scattering mechanisms and impurity or defect energy levels by means of low temperature Hall-effect measurements, employing a double-dewar cryostat. Measurement of the carrier mobility and concentration in the epitaxial semiconductor films being grown at any given time provides valuable information about the nature of the epitaxial growth mechanisms on the insulating substrates, the degree of control over the deposition processes, and the directions to be taken next by the materials studies.

Electrical characterization of the GaAs/ $Al_2O_3$  or GaAs/spinel systems is usually carried out on a "bridge sample" etched in the epitaxial layer by standard photolithographic techniques. Attempts to use the van der Pauw technique on the same layers have been found to be unsatisfactory. A group of twenty samples, grown by both the  $H_2$  and the He process, was measured by the two techniques. The resistivity measured by the van der Pauw method appeared to be within ~5 percent of the values obtained by the bridge measurements; however, the measured carrier concentrations were found to be consistently 25-40 percent high. Since this leads to errors in mobility on the order of 40 percent, the van der Pauw measurement technique has been discontinued, except for the measurement of GaAs films grown on semi-insulating GaAs. The reasons for the discrepancy are not fully understood, since the contacts were placed in a symmetrical fashion on the edges of a sample whose dimensions were typically much larger than the size of the contacts. Although inhomogeneities in film properties, particularly near the edges, could be a possible cause for variation between the two techniques, such a consistent difference for a large group of samples would probably not be expected. Further studies are now in progress to find the origin of the discrepancies.

## RESULTS AND DISCUSSION

Significant progress has been made in a number of areas related to the growth of GaAs on insulating substrates. In other areas only preliminary studies have been undertaken, but considerable insight into the understanding of the nucleation and growth of GaAs has been obtained. The sections below describe in detail the primary areas of study during the contract period and the progress that has been made.

### Film Properties

Effect of changes in deposition parameters. -- Emphasis was placed during the first part of the contract on the growth of undoped GaAs/ $Al_2O_3$  samples in order to determine the optimum growth rates and optimum flow rates of the various constituent gases. Films were grown on (0001)  $Al_2O_3$  at various temperatures between 650 and 700C with a wide variety of  $AsH_3$  and TMG concentrations. Experimentally, it is convenient to express the concentrations of  $AsH_3$ , TMG and dopant gases by flowmeter readings, given in cubic centimeters per minute (cc/min). As an example, in the data to be presented below, the notation 45-22-0 refers to an experiment in which the carrier gases were mixed with 45 cc/min of 10 percent  $AsH_3$ -in- $H_2$  and 22 cc/min of  $H_2$  which was bubbled through TMG (equilibrated at 0C). The last number, in this case 0, refers to the amount of dopant gas added, if any. The  $AsH_3$ :TMG mole ratio in this case is 3.5 (0.2 mmole of  $AsH_3$  to 0.058 mmole TMG). For the initial experiments the flow rate of pure  $H_2$  (or He) gas was fixed at 1.5 liters/min; in later studies this flow was increased to 3 liters/min.

As discussed in the contract proposal and demonstrated again during the course of the contract program, undoped GaAs films grown on  $Al_2O_3$  by the CVD method used here have always appeared to be p-type for the first few microns of growth. During subsequent growth the films become n-type and higher in quality as the thickness of the film increases. (This behavior will be discussed in more detail in a later section.) since the electrical properties of the films are changing with thickness, the measured electrical parameters are necessarily "averages" over the thickness of the film. In general, the outermost layers of the film will, therefore, have properties superior to the "average" value, and the layers nearer the interface will have inferior properties.

The growth of a high quality film was found to depend on the flow rates of the constituent gases through the reactor. The electrical measurements made on a number of films for various growth conditions are shown in Tables I through IV.

The effects of changing the  $AsH_3$  flow at constant TMG flow rates (at 650-660C) for various thicknesses are shown in Table I. The carrier concentration has been found to be dependent on the  $AsH_3$  flow rate for a given temperature and a fixed rate of  $H_2$  flow through TMG. For the higher  $AsH_3$  flow rates the carrier concentration saturates at some value characteristic of the gases used (see section below on effects of starting materials). As the  $AsH_3$  flow is reduced, the net carrier concentration also tends to

TABLE I  
ELECTRICAL PROPERTIES OF EPITAXIAL (111) GaAs/(0001) Al<sub>2</sub>O<sub>3</sub>  
AS A FUNCTION OF AsH<sub>3</sub> CONCENTRATION AND  
FILM THICKNESS AT 650-660C

Deposition Conditions* (AsH <sub>3</sub> -TMG-Dopant)	Thickness ( $\mu$ m)	$\rho$ (Ohm-cm)	Carrier Concentration (cm <sup>-3</sup> )	$\mu$ H (cm <sup>2</sup> /V-sec)
10-10-0	13.9	0.099	$1.35 \times 10^{18}$	47 (p-type)
20-10-0	10.9	55.2	$\sim 2 \times 10^{15}$	50 (p-type)
45-10-0	7.9	20.6	$\sim 3 \times 10^{15}$	100 (n-type)
90-10-0	12.0	0.345	$6.4 \times 10^{15}$	2840 (n-type)
90-10-0	29.5	0.169	$8.4 \times 10^{15}$	4400 (n-type)
20-22-0	4.0	0.02	$1.2 \times 10^{19}$	26 (p-type)
45-22-0	7.0	13.2	$1.3 \times 10^{16}$	36 (p-type)
90-22-0	8.2	0.42	$8.5 \times 10^{15}$	1750 (n-type)
90-22-0	10.5	0.10	$2.3 \times 10^{16}$	2940 (n-type)
90-22-0	18.3	0.28	$6.8 \times 10^{15}$	3280 (n-type)
180-22-0	21.8	0.15	$1.2 \times 10^{16}$	3740 (n-type)
180-45-0	10.9	0.15	$1.1 \times 10^{16}$	4050 (n-type)
180-45-0	11.5	0.10	$1.5 \times 10^{16}$	4150 (n-type)
180-45-0	15.6	0.15	$1.1 \times 10^{16}$	3890 (n-type)
250-45-0	16.4	0.27	$7.2 \times 10^{15}$	3200 (n-type)
180-60-0	18.5	24.5	$2.7 \times 10^{15}$	95 (p-type)
250-60-0	16.4	0.27	$7.2 \times 10^{15}$	3200 (n-type)

\*See text, p. 8, for significance of numbers.



TABLE II  
ELECTRICAL PROPERTIES OF EPITAXIAL (111) GaAs/(0001) Al<sub>2</sub>O<sub>3</sub>  
AS A FUNCTION OF TMG CONCENTRATION AND  
FILM THICKNESS AT 650-660 C

Deposition Conditions* (AsH <sub>3</sub> -TMG-Dopant)	Thickness (μm)	ρ (Ohm-cm)	Carrier Concentration (cm <sup>-3</sup> )	μ <sub>H</sub> (cm <sup>2</sup> /V-sec) (n-type)
90-5-0	15.5	0.189	1 x 10 <sup>16</sup>	3300
90-10-0	12.0	0.345	6 x 10 <sup>15</sup>	2840
90-10-0	29.5	0.169	8.4 x 10 <sup>15</sup>	4400
90-22-0	8.2	0.42	8.5 x 10 <sup>15</sup>	1750
90-22-0	10.5	0.1	2.3 x 10 <sup>16</sup>	2940
90-22-0	18.3	0.28	6.8 x 10 <sup>15</sup>	3280
90-30-0	20.3	0.43	5.8 x 10 <sup>15</sup>	2520
180-22-0	21.8	0.15	1.2 x 10 <sup>16</sup>	3740
180-35-0	15.4	0.11	1.2 x 10 <sup>16</sup>	4650
180-35-0	23.9	0.1	1.5 x 10 <sup>16</sup>	4430
180-45-0	10.9	0.15	1.1 x 10 <sup>16</sup>	4050
180-45-0	11.5	0.1	1.5 x 10 <sup>16</sup>	4150
180-45-0	15.6	0.15	1.1 x 10 <sup>16</sup>	3890
180-60-0	18.5	24.5	2.7 x 10 <sup>15</sup>	95 (p-type)

\*See text, p. 8, for significance of numbers.

TABLE III  
ELECTRICAL PROPERTIES OF EPITAXIAL (111) GaAs/(0001) Al<sub>2</sub>O<sub>3</sub>  
AS A FUNCTION OF AsH<sub>3</sub> AND TMG CONCENTRATIONS AT 675 C

Deposition Conditions* (AsH <sub>3</sub> -TMG-Dopant)	Thickness ( $\mu\text{m}$ )	$\rho$ (Ohm-cm)	Carrier Concentration ( $\text{cm}^{-3}$ )	$\mu_H$ ( $\text{cm}^2/\text{V-sec}$ )
45-22-0	~39	1.29	$3.4 \times 10^{16}$	142 (p-type)
90-22-0	25.4	0.21	$7.9 \times 10^{15}$	3720 (n-type)
180-22-0	17.4	0.35	$7.0 \times 10^{15}$	2530 (n-type)
250-22-0	22.9	0.12	$1.1 \times 10^{16}$	4560 (n-type)
150-35-0	11.2	1.11	$3.8 \times 10^{15}$	1500 (n-type)
180-35-0	11.7	0.65	$5.1 \times 10^{15}$	1900 (n-type)
250-35-0	8.6	0.14	$1.2 \times 10^{16}$	3610 (n-type)
250-22-0	22.9	0.12	$1.1 \times 10^{16}$	4560 (n-type)
250-35-0	24.4	0.11	$1.3 \times 10^{16}$	4400 (n-type)
250-45-0	20.5	0.08	$1.6 \times 10^{16}$	4530 (n-type)
250-60-0	18.9	0.12	$1.3 \times 10^{16}$	4000 (n-type)

\*See text, p. 8, for significance of numbers.

TABLE IV  
ELECTRICAL PROPERTIES OF EPITAXIAL (111) GaAs/(0001) Al<sub>2</sub>O<sub>3</sub>  
AS A FUNCTION OF TMG AND AsH<sub>3</sub> CONCENTRATIONS AT 700 C

Deposition Conditions* (AsH <sub>3</sub> -TMG-Dopant)	Thickness (μm)	ρ (Ohm-cm)	Carrier Concentration (cm <sup>-3</sup> )	μ <sub>H</sub> (cm <sup>2</sup> /V-sec)
250-35-0	19.2	0.24	7.4 x 10 <sup>15</sup>	1940 (n-type)
325-35-0	13.7	0.31	8.8 x 10 <sup>15</sup>	3470 (n-type)
325-35-0	13.7	0.21	8.8 x 10 <sup>15</sup>	3470 (n-type)
325-45-0	13.7	0.11	1.3 x 10 <sup>16</sup>	2800 (n-type)
325-60-0	10.0	0.21	1.1 x 10 <sup>16</sup>	3210 (n-type)
250-60-0	12.5	0.19	1.0 x 10 <sup>16</sup>	3210 (n-type)

\*See text, p. 8, for significance of numbers.

decrease. With continued decrease in  $\text{AsH}_3$ , the films eventually became p-type, and the quality of the films appears visually to deteriorate at very low  $\text{AsH}_3$  concentrations. This behavior was examined for a variety of growth conditions, and it was found that p-type films could be produced in this manner with net hole concentrations ranging from  $\sim 3 \times 10^{15}$  to  $\sim 10^{19} \text{cm}^{-3}$ . These effects may be due to As deficiencies in the films.

The effects of changing TMG flow rate at constant  $\text{AsH}_3$  rate (at  $\sim 650$ - $660^\circ\text{C}$ ) for films of various thickness are shown in Table II. In general it is found that the higher flow rates of TMG, and hence faster deposit growth rates, produce superior quality films. Increasing the concentration ratio of Ga to As by increasing the TMG rate to a very high value (for constant  $\text{AsH}_3$  rate) again leads to a p-type film as evidenced by the last sample in the table.

As the growth temperature is increased it is found that higher  $\text{AsH}_3$  rates are needed to produce a more reflective film. The properties of several films grown at  $675$  and  $700^\circ\text{C}$  are shown in Tables III and IV. The necessary flow rates of  $\text{AsH}_3$  range from  $\sim 180$  cc/min at  $650^\circ\text{C}$  to  $\sim 325$  cc/min at  $700^\circ\text{C}$ . A flow rate of  $35$ - $45$  cc/min of  $\text{H}_2$  passing over TMG usually yields good quality films over the whole temperature range from  $650$  to  $700^\circ\text{C}$  for films  $>10 \mu\text{m}$  thick.

Effect of different starting materials. -- Considerable attention has been given to the question of the effect of the impurity content and chemical species of the reactants upon the properties of the GaAs layers.

$\text{H}_2$  process. -- Electrical data on samples grown more recently by the  $\text{H}_2$  process using the optimized flow rates described above are shown in Table V. The reasons for gross differences between these data and those given in the preceding tables are primarily associated with differences in starting materials; this will be discussed in more detail below. Note that the mobilities are nearly those of good bulk GaAs of the same carrier concentration, for these thick samples.

He process. -- During the later stages of the contract program, He has been investigated as a substitute for  $\text{H}_2$  as a carrier gas in the CVD process. Initially, five-9s-purity He gas was substituted for the  $\text{H}_2$  carrier, keeping the  $\text{AsH}_3$ - $\text{H}_2$  mixture as the source of  $\text{AsH}_3$ . The electrical properties of this series of films are shown in Table VI.

Next, 10 percent  $\text{AsH}_3$ -in-He was substituted for the  $\text{AsH}_3$ - $\text{H}_2$  mixture. The properties of these films, as shown in Table VII, were found to change little from those obtained previously; however, the mobilities of the later samples in this group were found to be considerably improved. This appeared to be a consequence of an extra purification step for the TMG.

TABLE V  
ELECTRICAL PROPERTIES OF EPITAXIAL (111) GaAs/(0001) Al<sub>2</sub>O<sub>3</sub>  
GROWN USING H<sub>2</sub> AS CARRIER GAS AND TEN PERCENT  
AsH<sub>3</sub> IN H<sub>2</sub>

Growth Conditions* (AsH <sub>3</sub> -TMG-Dopant)	Temp (C)	Thickness ( $\mu$ m)	$\rho$ (Ohm-cm)	Carrier Concentration (cm <sup>-3</sup> )	$\mu$ H (cm <sup>2</sup> /V-sec) (n-type)
250-45-0	675	23.8	0.0215	$6.58 \times 10^{16}$	4410
300-45-0	675	18.7	0.0234	$7.2 \times 10^{16}$	3710
300-45-0 (5 min) 200-45-0 (15 min)	675	19.0	0.0274	$5.2 \times 10^{16}$	4400
250-45-0	700	17.3	0.0191	$7.8 \times 10^{16}$	4180
300-45-0	700	20.0	0.0193	$7.8 \times 10^{16}$	4190
350-45-0	700	19.9	0.0170	$9.3 \times 10^{16}$	3970

\*See text, p. 8, for significance of numbers.

TABLE VI  
 ELECTRICAL PROPERTIES OF EPITAXIAL (111) GaAs/(0001) Al<sub>2</sub>O<sub>3</sub>  
 GROWN AT 700 C AND CONSTANT AsH<sub>3</sub> CONDITIONS, USING  
 FIVE-9s He AS CARRIER GAS AND TEN PERCENT AsH<sub>3</sub> IN H<sub>2</sub>

Growth Conditions* (AsH <sub>3</sub> -TMG-Dopant)	Thickness (μm)	ρ (Ohm-cm)	Carrier Concentration (cm <sup>-3</sup> )	μ <sub>H</sub> (cm <sup>2</sup> /V-sec) (n-type)
325-45-0	5.2	0.47	2.2 x 10 <sup>16</sup>	600
325-45-0	6.9	3.1	3.6 x 10 <sup>15</sup>	550
325-45-0	16.1	0.13	1.1 x 10 <sup>16</sup>	4450
325-45-0	24.6	0.27	7.6 x 10 <sup>15</sup>	3040
325-55-0	10.3	0.22	7.0 x 10 <sup>15</sup>	4000
325-65-0	10.7	0.18	1.1 x 10 <sup>16</sup>	3340
325-65-0	17.4	0.28	6.3 x 10 <sup>15</sup>	3870
325-75-0	23.5	0.35	5.4 x 10 <sup>15</sup>	3370
325-75-0	23.4	0.31	5.7 x 10 <sup>15</sup>	3650
325-85-0	16.4	0.13	1.4 x 10 <sup>16</sup>	3560
325-85-0	22.4	0.30	7.1 x 10 <sup>15</sup>	2940

\*See text, p. 8, for significance of numbers.

TABLE VII  
 ELECTRICAL PROPERTIES OF EPITAXIAL (111) GaAs/(0001) Al<sub>2</sub>O<sub>3</sub>  
 GROWN AT 700 C AND CONSTANT TMG, USING FIVE-9s He  
 AS CARRIER GAS AND TEN PERCENT AsH<sub>3</sub> IN He

Growth Conditions* (AsH <sub>3</sub> -TMG-Dopant)	Thickness (μm)	ρ (Ohm-cm)	Carrier Concentration (cm <sup>-3</sup> )	μ <sub>H</sub> (cm <sup>2</sup> /V-sec) (n-type)
325-45-0	8.7	0.26	1.0 x 10 <sup>16</sup>	2380
325-45-0	12.2	0.20	1.1 x 10 <sup>16</sup>	2790
325-45-0	20.8	0.21	9.5 x 10 <sup>15</sup>	3090
325-45-0	24.3	0.17	9.9 x 10 <sup>15</sup>	3810
450-45-0	9.5	0.36	8.0 x 10 <sup>15</sup>	2150
450-45-0	10.3	0.28	8.4 x 10 <sup>15</sup>	2700
450-45-0	11.3	0.21	9.8 x 10 <sup>15</sup>	3060
600-45-0	11.7	0.14	1.1 x 10 <sup>16</sup>	3960
750-45-0	11.9	0.30	1.7 x 10 <sup>16</sup>	3470
450-45-0	25.3	0.11	1.2 x 10 <sup>16</sup>	4650
450-45-0	26.7	0.083	1.3 x 10 <sup>16</sup>	5590 13000 (77K)
600-45-0 (5 min) 450-45-0 (4 min) 400-45-0 (21 min)	17.0	0.10	1.3 x 10 <sup>16</sup>	4960

\*See text, p. 8, for significance of numbers.

Prior to the evaluation of these "good" samples, the six-9s-purity He carrier gas was installed and the excellent results shown in Table VIII led to the conclusion that this high-purity carrier gas was responsible for the high quality samples. Subsequent investigation, however, showed that the five-9s He apparently contaminated the TMG after continuous use. A short distillation at 0C returned the TMG to a purity which yielded good quality films. The six-9s He, on the other hand, does not apparently contaminate the TMG source, as no further purification steps have been found necessary to produce excellent quality films with this gas.

Reactant materials. -- Considerable effort has been devoted to investigating the effect of purity of various starting materials on the properties of the GaAs films. It has been found that n-type impurity concentrations from  $\sim 10^{15}$  to  $\sim 10^{17}$  cm<sup>-3</sup> can be obtained in films in which no dopant was intentionally added during growth. The primary factor in determining this concentration is the purity of the materials used to grow the films. The impurity concentration is measured by growing thick films under optimum growth conditions; since there is little variation in film properties for films thicker than 15-20 $\mu$ m, the measured impurity concentration can be a good indication of the quality of the starting materials.

TABLE VIII  
ELECTRICAL PROPERTIES OF EPITAXIAL (111) GaAs/(0001) Al<sub>2</sub>O<sub>3</sub>  
GROWN UNDER DIFFERENT CONDITIONS, USING SIX-9s He AS  
CARRIER GAS AND TEN PERCENT AsH<sub>3</sub> IN He

Growth Conditions* (AsH <sub>3</sub> -TMG-Dopant)	Temp (C)	Thickness ( $\mu$ m)	$\rho$ (Ohm-cm)	Carrier Concentration (cm <sup>-3</sup> )	$\mu_H$ (cm <sup>2</sup> /V-sec) (n-type)
400-45-0 (5 min) 225-45-0 (55 min)	675	26.4	0.15	$7.9 \times 10^{15}$	5230
600-45-0 (6 min) 400-45-0 (27 min)	700	18.6	0.12	$1.1 \times 10^{16}$	4330
600-45-0 (2 min) 400-45-0 (4 min) 275-45-0 (54 min)	700	52.0	0.15	$6.2 \times 10^{15}$	6230 19,300 (77K)
400-45-0 (30 min)	700	14.3	0.11	$1.2 \times 10^{16}$	4560
400-45-0 (30 min)	725	19.5	0.14	$1.1 \times 10^{16}$	4360
400-45-0 (30 min)	750	23.8	0.18	$9.6 \times 10^{15}$	3527

\*See text, p. 8, for significance of numbers.



At the present time it is not possible to predict what impurity concentrations will result from a given set of starting materials. It has been determined that the dominant source of impurity can be either the TMG or the AsH<sub>3</sub> and, to a lesser extent, the carrier gas. In addition, the purity of the starting material may vary considerably from tank to tank even though the vendor's purity specifications are the same.

The lowest carrier concentrations so far obtained in thick samples have been  $\sim 10^{15}$  cm<sup>-3</sup>, grown in the H<sub>2</sub> system using a particular batch of TMG, made from four-9s Ga, and an AsH<sub>3</sub>-in-H<sub>2</sub> mixture. The mobility for this carrier concentration was  $\sim 3000$ - $4000$  cm<sup>2</sup>/V-sec. In the He system, a batch of TMG made from six-9s Ga produced films with carrier concentrations in the mid- $10^{15}$  range and mobilities in the same range as those above. More typically, the TMG and AsH<sub>3</sub> which have been used yield films with  $n \sim 10^{16}$  -  $10^{17}$  cm<sup>-3</sup> and mobilities approaching that of bulk material. For example, the mobility value of over  $6000$  cm<sup>2</sup>/V-sec (and  $19,000$  cm<sup>2</sup>/V-sec at 77K) shown in Table VIII for a film  $\sim 50\mu$  m thick is evidence of very high quality GaAs.

Mobility variation with carrier concentration. -- All of the updoped samples grown during the first quarter of the contract were grown by the H<sub>2</sub> process. The variation of the mobility of these samples with carrier concentration is plotted in Figure 2. The data have been divided according to growth temperature, and from these data it appears that there is no definite correlation between mobility and growth temperatures of 650-700C. (It should be noted that these data represent samples grown over a wide range of growth conditions and are not optimized properties.)

Similar electrical data on the GaAs/Al<sub>2</sub>O<sub>3</sub> films grown by the H<sub>2</sub> process during the latter part of the contract are shown in Figure 3. Here the data have been separated according to the quality of the starting materials and are reported for films greater than  $10\mu$  m thick. Basically the same quality TMG (made from four-9s Ga) has been used for all, and the different data points correspond to different tanks of AsH<sub>3</sub>. It can be seen that the carrier concentration varies by nearly two orders of magnitude.

Mobility-versus-carrier concentration data on the films grown more recently by the He process are shown in Figure 4. These data are similarly divided according to starting materials; however, in this case, the variation of carrier concentration reflects primarily the quality of the TMG. Changing the available AsH<sub>3</sub>-in-He tanks appeared to make little difference, and changing the He carrier gas from six-9s to four-9s purity resulted only in the small differences between the solid circles and open squares. The carrier concentration is again found to vary over two orders of magnitude, illustrating the importance of high quality TMG as well as AsH<sub>3</sub> in producing films of lower carrier concentration. That there are still considerable impurities or defects in the films with low carrier concentrations is suggested by the depression of mobility for carrier concentrations approaching  $10^{15}$  cm<sup>-3</sup>.

Variation of properties with thickness. -- As mentioned above, the region of the first few microns of growth of an updoped sample is p-type. With subsequent growth the sample reverts to n-type with a net donor concentration characteristic of growth conditions and especially of the gases used for source materials. An extensive study of the first few microns of growth was begun recently, using the available TMG (made from four-9s Ga) and AsH<sub>3</sub>-in-H<sub>2</sub>. A group of samples ranging in thickness from  $\sim 0.2$  to  $1.7\mu$  m and grown with constant growth conditions typically exhibited p-type carrier

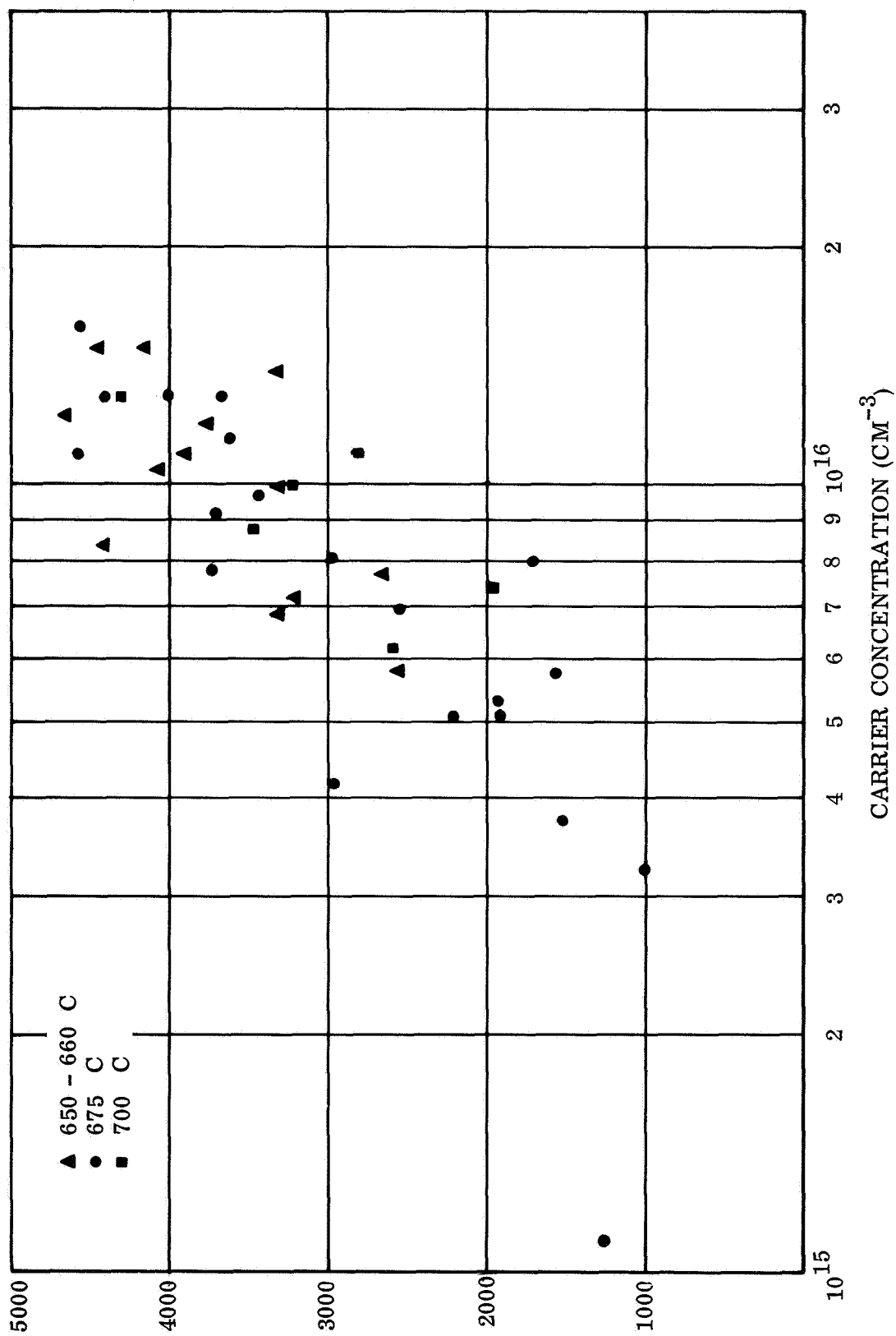


Figure 2. Mobility vs Carrier Concentration for GaAs/Al<sub>2</sub>O<sub>3</sub>, Undoped Samples (Thickness Range: 4-30 μm)

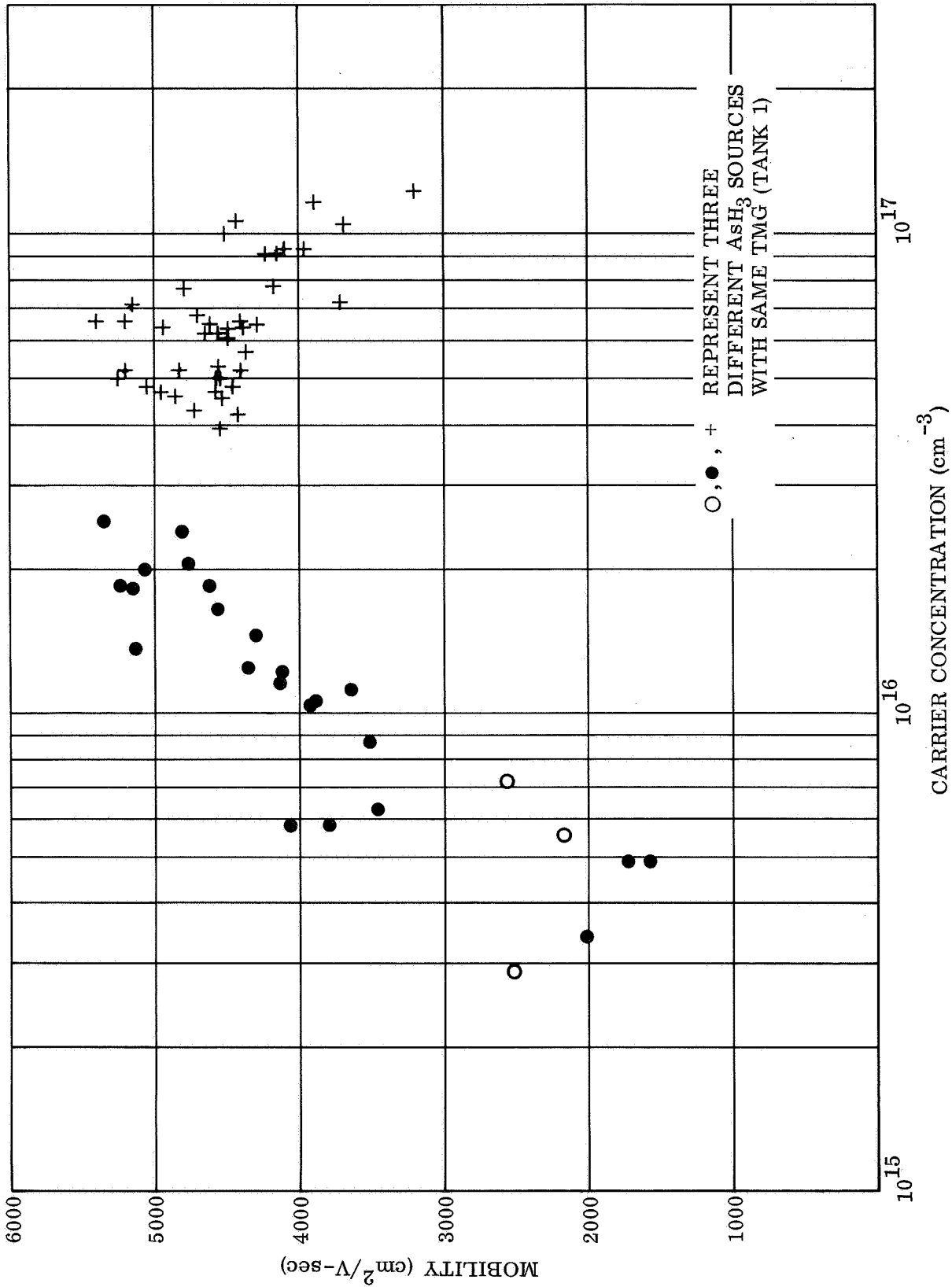
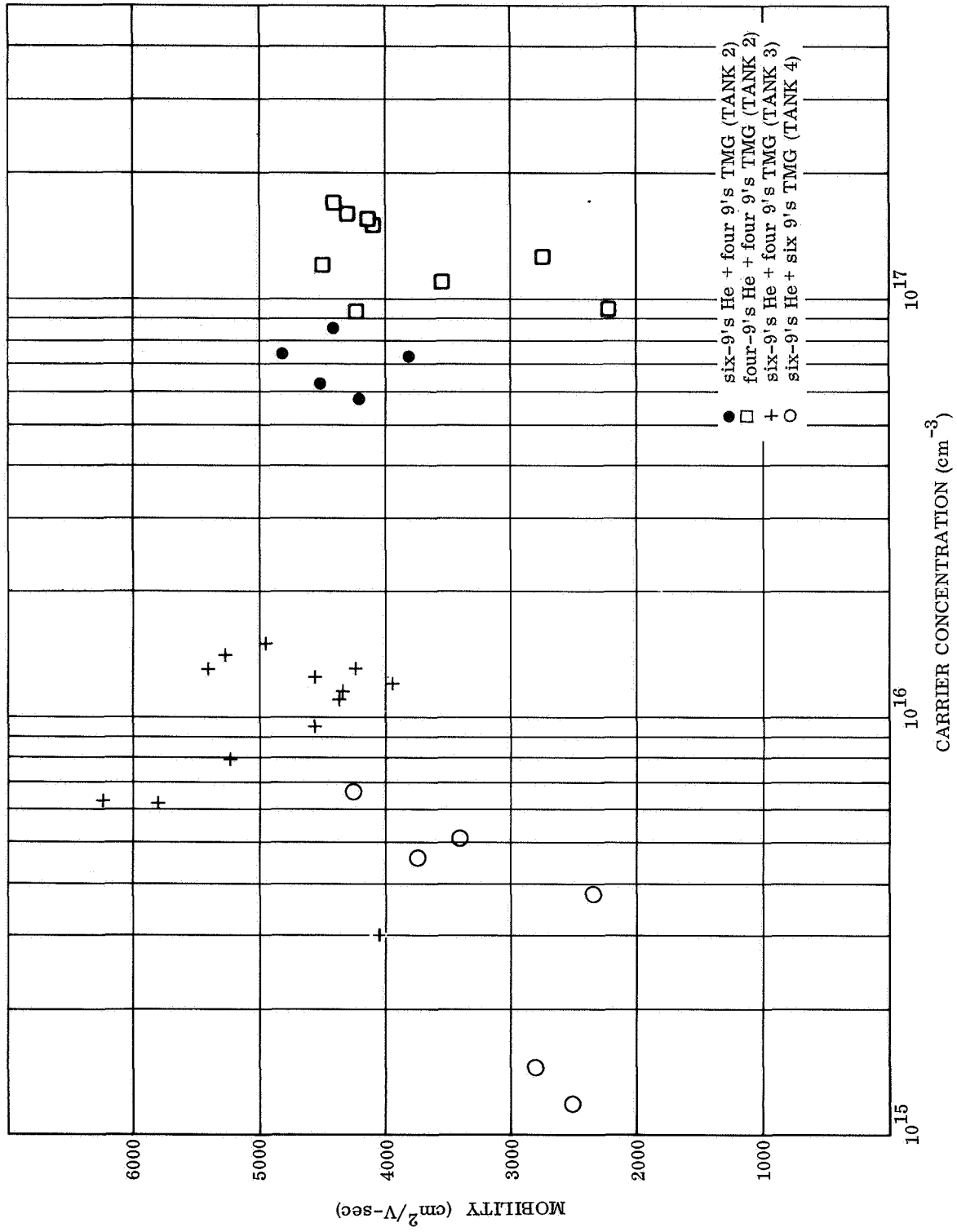


Figure 3. Mobility vs Carrier Concentration for GaAs/Al<sub>2</sub>O<sub>3</sub> Undoped Samples (Thickness > 10μm) — H<sub>2</sub> Process



concentrations between  $10^{17}$  and  $10^{18}$   $\text{cm}^{-3}$ . If growth is continued to  $\sim 5\mu\text{m}$ , the measured (average) p-type carrier concentration is lowered to the mid- $10^{16}$  range. By  $8\mu\text{m}$  thickness the films convert to n-type with a measured concentration of  $\sim 10^{15}$   $\text{cm}^{-3}$ . For the particular growth conditions used, a thick film ( $>15\mu\text{m}$ ) exhibited a net n-type carrier concentration of  $3-5 \times 10^{15}$   $\text{cm}^{-3}$ . If one assumes the n-type impurities are present in the film from the start of growth, it is apparent that the thickness of the p-layer will be a function of the n-type impurity concentration in the system. If a thick film exhibits an n-type doping level  $\sim 10^{17}$   $\text{cm}^{-3}$ , for example, the p-layer will probably be only one or two microns thick.

Once the film has converted to n-type the carrier concentration rises rapidly to the thick-film value. The mobility tends to continue to improve as the film becomes thicker, usually "saturating" by the time the film has grown to  $\sim 15-20\mu\text{m}$ . The electrical properties of a series of films grown at constant growth conditions with different thicknesses are shown in Table IX.

Studies of the gray stage. -- A characteristic of the GaAs films that have been grown by the CVD process is the occurrence of a "gray stage" during the first few minutes of growth, in which the film is gray and dull in appearance. The length of time the film is in the gray stage is found to depend on the flow rates of the constituent gases through the reactor. In general, higher than "normal"  $\text{AsH}_3$  flow rates result in a longer gray stage; lower  $\text{AsH}_3$  flow rates than "normal" (under conditions that provide thick n-type films) or increased carrier gas flow tends to shorten the gray stage. These results, together with the fact that a reactor of narrower design inhibits the gray stage, suggest that this behavior may be related to the flow patterns and turbulence of the gases passing through the reactor. Alternatively, the gray stage may be a consequence of the  $\text{AsH}_3$ -TMG ratio present in the reactor at any particular stage of growth. This intermediate gray stage is observed in both the  $\text{H}_2$  and the He systems and appears to be a beneficial concomitant for the production of smooth, highly reflective surfaces on the GaAs layers.

Electrical measurements have shown that the gray stage is not related to the p-type layer discussed above, and seems to have little effect on the overall electrical quality of thick films. A series of GaAs/ $\text{Al}_2\text{O}_3$  films was grown (in  $\text{H}_2$ ) in which various thicknesses of the gray stage growth were allowed to continue before the TMG- $\text{AsH}_3$  ratio was altered to terminate the gray stage and effect reflective film growth. The gray stage was controlled for various lengths of time ranging from 1 minute to 20 minutes of growth. The electrical parameters of this series of films are shown in Table X. Based on the average mobility values obtained, there does not appear to be a difference in quality among the films, suggesting that the gray appearance of the films during growth is not a primary factor in the electrical properties of the films.

From preliminary studies of the growth of GaAs on Cr-doped GaAs, it was found that the gray stage can also be induced in the homoepitaxial material and is thus not peculiar to growth on insulators.

Impurity concentration. -- It is evident from the electrical data on undoped GaAs films grown by the CVD process that the limitations in mobility are related in great part to unwanted impurities present in the films. That a considerable portion of these limitations results from impurities in the gases used to grow the films has been

TABLE IX  
ELECTRICAL PROPERTIES OF EPITAXIAL (111) GaAs/(0001) Al<sub>2</sub>O<sub>3</sub>  
AS A FUNCTION OF LAYER THICKNESS FOR A GIVEN  
AsH<sub>3</sub>-TMG RATIO (250-35-0)\* AT 675 C

Thickness ( $\mu$ m)	$\rho$ (Ohm-cm)	Carrier Concentration (cm <sup>-3</sup> )	$\mu_H$ (cm <sup>2</sup> /V-sec)
0.9	$\geq 10^4$	†	- (p-type)
2.9	$4.3 \times 10^3$	†	- (n-type)
4.5	0.46	$\sim 8.0 \times 10^{15}$	1690 (n-type)
7.3	0.26	$8.1 \times 10^{15}$	2950 (n-type)
8.6	0.14	$1.2 \times 10^{16}$	3610 (n-type)
19.6	0.13	$1.3 \times 10^{16}$	3630 (n-type)
24.4	0.11	$1.3 \times 10^{16}$	4400 (n-type)

\*See text, p. 8, for significance of numbers.

demonstrated. It is probable that in addition there are impurities present on the Al<sub>2</sub>O<sub>3</sub> surface which can influence the interface layer. Also the defect structure near the interface may contribute electrically-active species deleterious to the quality of the GaAs.

The dominant impurity (or impurities) evident in thick undoped films grown by either the H<sub>2</sub> or the He process is a donor; since there is little change in the carrier concentration at 77K from that at 300K, it is apparent that the energy associated with this impurity is very small, the level probably being less than 0.005eV from the conduction band. Measurements of the carrier concentration as a function of temperature over the temperature range from 63 to 300K verify this conclusion and are shown in Figure 5. The carrier concentration is seen to decrease by less than 30 percent in this temperature range, indicating that the donor is still nearly completely ionized at 63K. This sample was grown by the He process and is of reasonably good quality, as evidenced by a room temperature mobility of 5400 cm<sup>2</sup>/V-sec and 77K mobility of 12,500 cm<sup>2</sup>/V-sec.

The only donor impurities having unambiguously established levels this shallow in GaAs are Se, Te, Si, Ge, Sn and probably S. Without knowing the exact preparation and handling techniques used in the production of the various quantities of TMG and AsH<sub>3</sub> used in this work, it is not possible to predict which impurities would be present; however, from the spectrographic analyses available on samples of TMG, it is known that Si is present as a major impurity (100-500 ppm) and hence would be one of the most likely possibilities.

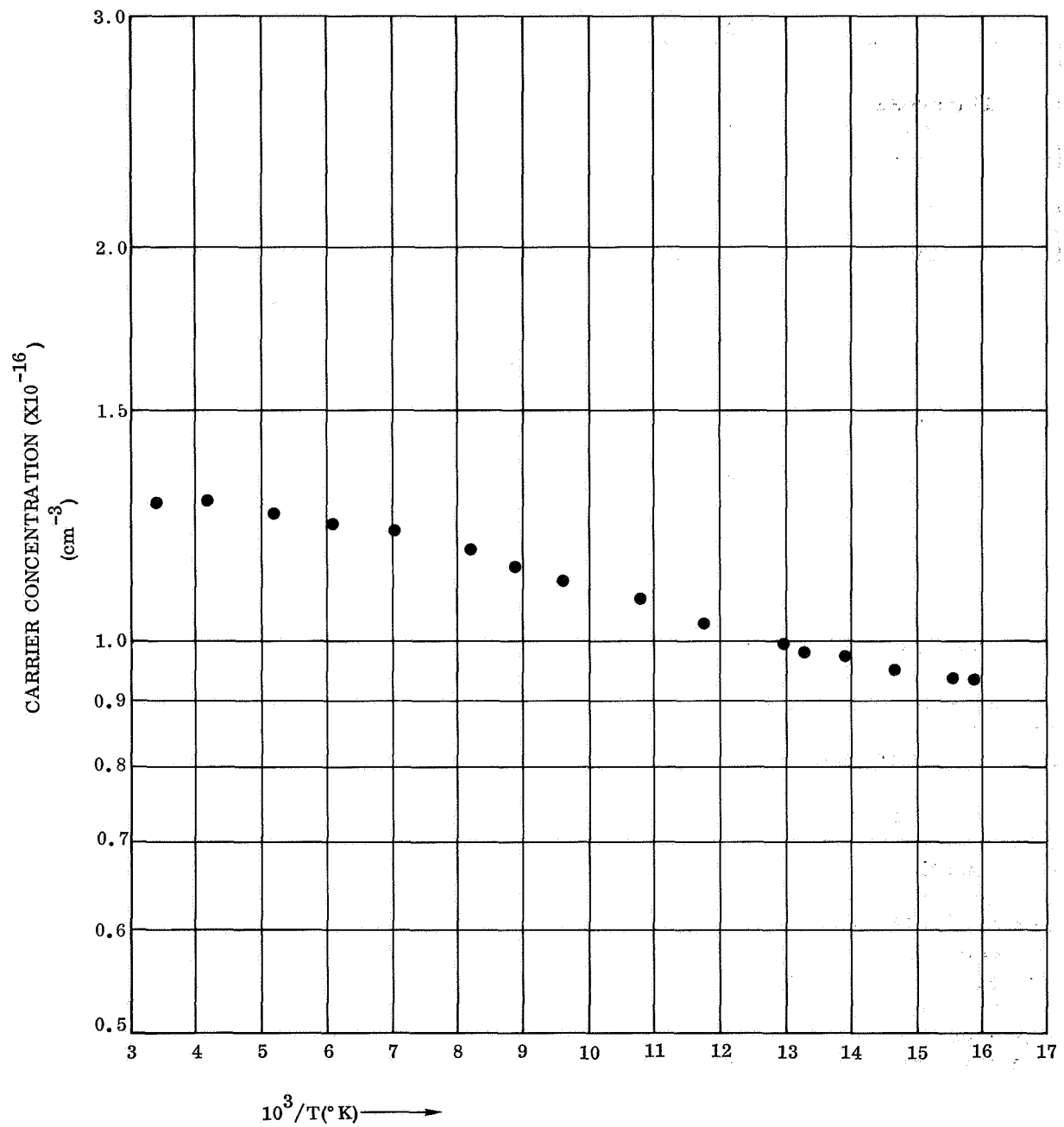


Figure 5. Variation of Carrier Concentration with Reciprocal Temperature for an Undoped GaAs/Al<sub>2</sub>O<sub>3</sub> Film

TABLE X  
STUDY OF THE FORMATION AND EFFECT OF THE GRAY STAGE  
AT 675 C IN AN H<sub>2</sub> ATMOSPHERE

Growth Conditions* (AsH <sub>3</sub> -TMG-Dopant)	Time of Growth (min)	Thickness (μm)	Observations During Growth	ρ (Ohm-cm)	Carrier Concentration (cm <sup>-3</sup> )	μ H (cm <sup>2</sup> /V-sec)
250-45-0	31	28.0	Gray 1 min, then cleared	0.0623	1.98 x 10 <sup>16</sup>	5070
300-45-0	20	19.0	Gray for 3-4 min	0.0728	1.86 x 10 <sup>16</sup>	4620
300-45-0	22	21.7	Started to clear in 5 min	0.0664	1.83 x 10 <sup>16</sup>	5140
325-45-0 (2 min)	20	19.2	Gray for 6 min	0.0830	1.65 x 10 <sup>16</sup>	4560
370-45-0 (4 min)	20	20.8	Gray for 11 min	0.0642	1.85 x 10 <sup>16</sup>	5250
210-45-0 (14 min)	22	22.6	Gray for 15 min	0.0462	2.53 x 10 <sup>16</sup>	5350
325-45-0 (10 min)	20	18.9	Gray first 4 min, Clear 5-8 min total	0.0642	2.05 x 10 <sup>16</sup>	4760
210-45-0 (10 min)	20	22.0	Gray 8-15 min total Clear 16-20 min total	0.0542	2.41 x 10 <sup>16</sup>	4800
300-45-0	20	22.0	1/2 sample--gray and cleared near end of run 1/2 sample--gray entire run	0.0987	1.47 x 10 <sup>16</sup>	4300

\*See text, p. 8, for significance of numbers.



The reduction in mobility at low carrier concentrations in thick samples suggests that the films are partially compensated. Although the origin of any acceptors is unknown, such impurities could very likely occur in the gases. The role of defects in GaAs is not well understood, but the formation of defects or defect-impurity complexes could conceivably provide another compensating mechanism. In addition to the above, GaAs is known to exhibit anomalous mobility effects which can be associated with inhomogeneous distributions of impurities. Such distributions, by creating space-charge regions in the semiconductor, lead to scattering centers quite effective in reducing the mobility in GaAs.

The changes in electrical properties of the p-type layer near the  $Al_2O_3$ -GaAs interface between 300 and 77K are very similar to those discussed above. Measurements of the electrical properties of the first few microns of growth at low temperature indicate the existence of a very shallow acceptor level which is still ionized at 77K. The origin of such a shallow level is at present not known. Since the defect structure is highest at the interface and the acceptor concentration appears to decrease with distance from the interface, it is possible that the acceptor is related to this defect structure. Impurities on the  $Al_2O_3$  surface also can contribute to the electrical behavior in the first few microns of thickness; however, preliminary experiments have indicated that different cleaning procedures do not lead to significant differences in the p-type layer. It would thus appear that residual impurities are at least not the dominant factor in determining the p-type behavior.

The growth of GaAs on semi-insulating GaAs substrates has been examined only in a preliminary fashion. A thin ( $\sim 3.5\mu m$  thick) film was found to be n-type with  $n \sim 3 \times 10^{15} \text{ cm}^{-3}$  and  $\mu \sim 3200 \text{ cm}^2/\text{V-sec}$ . This is indicative of the relatively higher quality of the homoepitaxial material during the first few microns of growth. Beveling and staining this sample revealed an interface layer approximately  $1\mu m$  thick; however, the electrical conductivity type of this layer was not determined. Further studies of the characteristics of GaAs layers in the early stages of growth on GaAs substrates would be of considerable importance in understanding the interface problem.

A thicker ( $\sim 48\mu m$ ) film of GaAs on GaAs was found to exhibit a carrier concentration and mobility equivalent to GaAs/ $Al_2O_3$  growth ( $n \sim 10^{16} \text{ cm}^{-3}$ ,  $\mu \sim 5500 \text{ cm}^2/\text{V-sec}$ ). This suggests that the quality of thick GaAs growth on  $Al_2O_3$  is not limited by any problem related to heteroepitaxial growth, such as thermal expansion differences between GaAs and  $Al_2O_3$  or lattice mismatch at the interface.

Studies of the nucleation process. -- The quality of an epitaxial film is strongly dependent upon the nucleation process; therefore, investigation of the early stages of growth under different growth parameters has been regarded as valuable in optimizing the overall growth process. In situ recording of nucleation phenomena is not feasible in chemical vapor deposition equipment; however, the technique of "freezing" the growth at different stages and applying replica electron microscopy and reflection electron diffraction (RED) to examine the results supplies some of the same kind of information. The photomicrographs and RED patterns included here reveal some of the nature of the heteroepitaxial growth process for (111) GaAs on (0001)  $Al_2O_3$  (and probably on other insulating substrates which control (111) GaAs growth).

The growth conditions used for these studies were dictated by observations previously made for thick films ( $>20\mu\text{m}$ ) of GaAs grown on (0001)  $\text{Al}_2\text{O}_3$ , i.e., the highest mobilities obtained to date ( $\sim 5500\text{ cm}^2/\text{V}\text{-sec}$ ) were for films grown at about 675C when the growth rate approached 0.8-1 $\mu\text{m}$  per minute. Although the growth rate of the films for a given TMG concentration and given flow conditions did not change appreciably between 600-800C (Figure 6), RED patterns supported the observation that film growth was better at 675C than, for example, at 800C, as evidenced by the strong Kikuchi lines and untwinned pattern shown in Figure 7.

GaAs/(0001)  $\text{Al}_2\text{O}_3$  film formation was interrupted at different stages of the growth to study the nucleation process in a series of experiments. The effects of annealing on several selected films of this type were also studied. The results are quite informative and are described below.

Figure 8 shows replicas of the films produced at 675C by exposure to TMG- $\text{AsH}_3$  mixtures with  $\text{AsH}_3$ -TMG-dopant flowmeter settings of 250-45-0, respectively, for 1, 3, 5, and 7 sec. At 1 sec, the  $\text{Al}_2\text{O}_3$  surface seems to be almost completely covered by a host of individual medium-sized pyramid-shaped nuclei (about 0.15 $\mu\text{m}$  across) that are oriented in the same direction. The film surface is comparatively rough at this stage (average thickness of nucleus  $\sim 350\text{\AA}$ .) At 3 sec, the surface seems to have become quite smooth, but "islands" are evident, presumably openings of bare  $\text{Al}_2\text{O}_3$ . These openings appear to have filled in at the end of 5 sec, the surface remaining relatively smooth, but at 7 sec the surface has again become slightly roughened. The surface still appeared rough on a film grown for 10 sec (0.15 $\mu\text{m}$  thick) (Figure 9a), smoother after 20 sec of growth (0.3 $\mu\text{m}$  thick) (Figure 9b), and finally appeared quite smooth after a film of GaAs was grown for 30 sec (0.45 $\mu\text{m}$  thick) (Figure 9c).

The variation in the crystal quality of many of these thin films with changes in thickness and deposition parameters was also followed by RED (110) patterns. An examination of Figures 9(a-c) indicates that films formed during the first 10 sec of growth ( $<2000\text{\AA}$ ) possess varying degrees of twin structure; at 3000 $\text{\AA}$  (20 sec of growth), however, the pattern no longer displays the extra spots associated with twin structure.

RED patterns also showed the effect of using different  $\text{AsH}_3$ -TMG ratios and post-annealing steps on the quality of growth formed after 1 sec at a TMG flowmeter setting of 45. In Figure 10 considerable differences can be observed in the patterns for  $\text{AsH}_3$  flowmeter settings of 50 (a high density of strong extraneous spots), 150, 200, and 250 (weak twin spots present).

Figures 11 and 12 represent the results which were obtained when very dilute TMG- $\text{AsH}_3$  mixtures were pyrolyzed for film growth. These were produced by stabilizing the growth conditions (flowmeter settings of 250-45-0) at 675C, turning off the TMG for 15 sec, and diverting the  $\text{H}_2$  carrier so that only residual TMG in the line was directed into the reactor for 1 sec (Figure 11) and 6 min (Figure 12). Figure 11 reveals that the growth even at extreme gas dilutions can produce a multitude of very small uniformly-arranged nuclei ( $\sim 200\text{\AA}$  across) that almost cover the entire substrate surface.

If additional growth is essentially terminated and the temperature is maintained for several minutes, these nuclei may move and coalesce into relatively large (0.2 $\mu\text{m}$  across) oriented triangular islands with pyramidal structures (of the type) shown in Figure 12. Several of the crystallites seen in this figure have coalesced, and possess exterior shapes

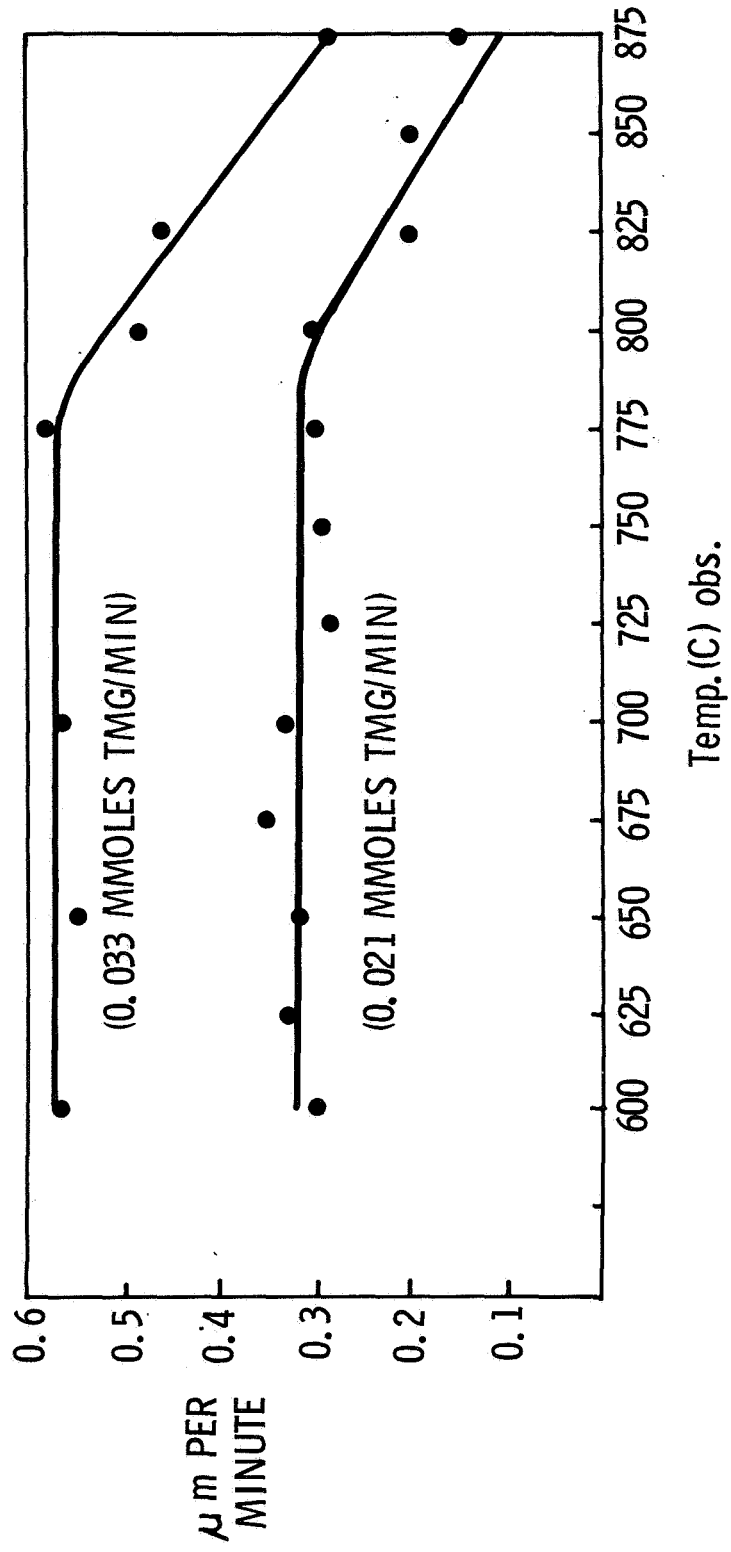
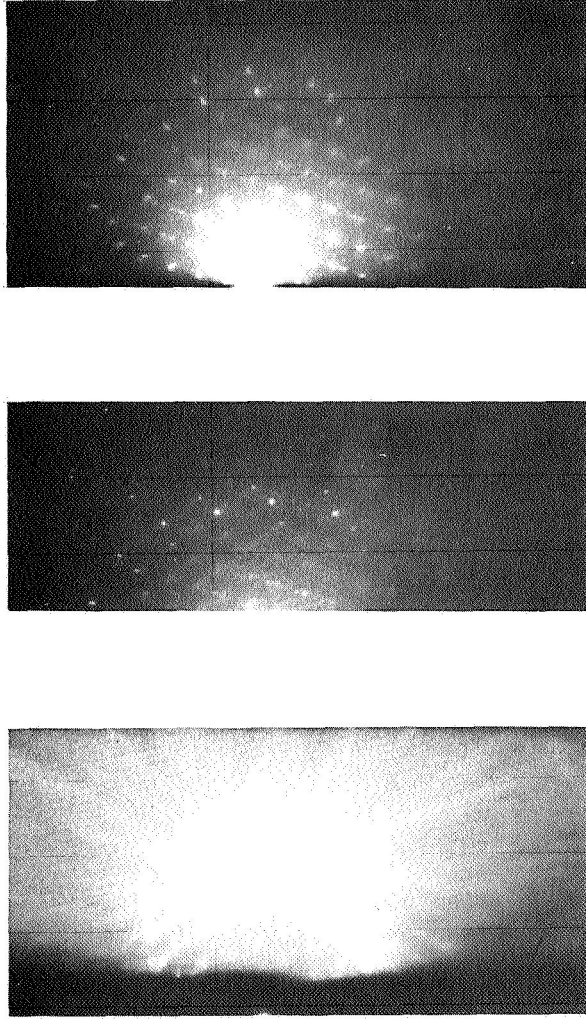
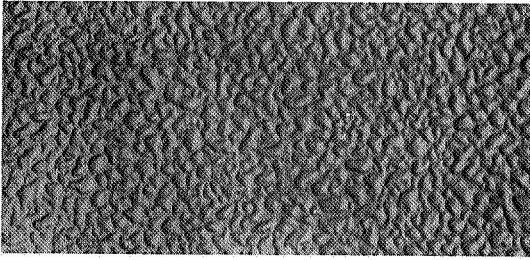


Figure 6. Effect of Substrate Temperature on Rate of Growth of (111) GaAs on (0001)  $\text{Al}_2\text{O}_3$

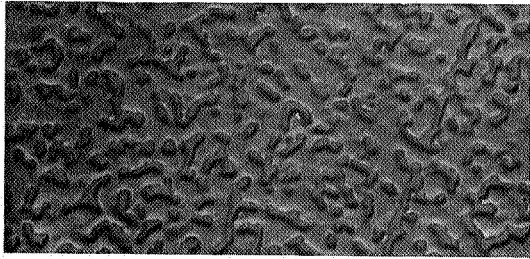


(a) (b) (c)

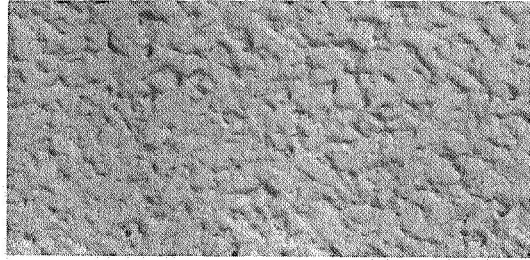
Figure 7. (110) XRD Photographs of (111) GaAs/(0001)  $Al_2O_3$  Films Grown at (a) 675C; (b) 800C; (c) 825C



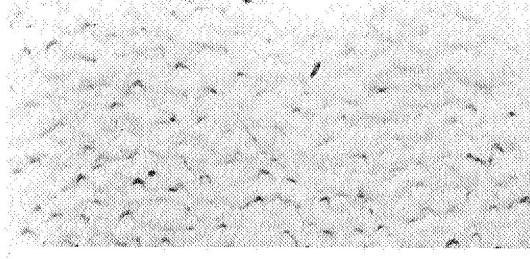
(a)



(b)

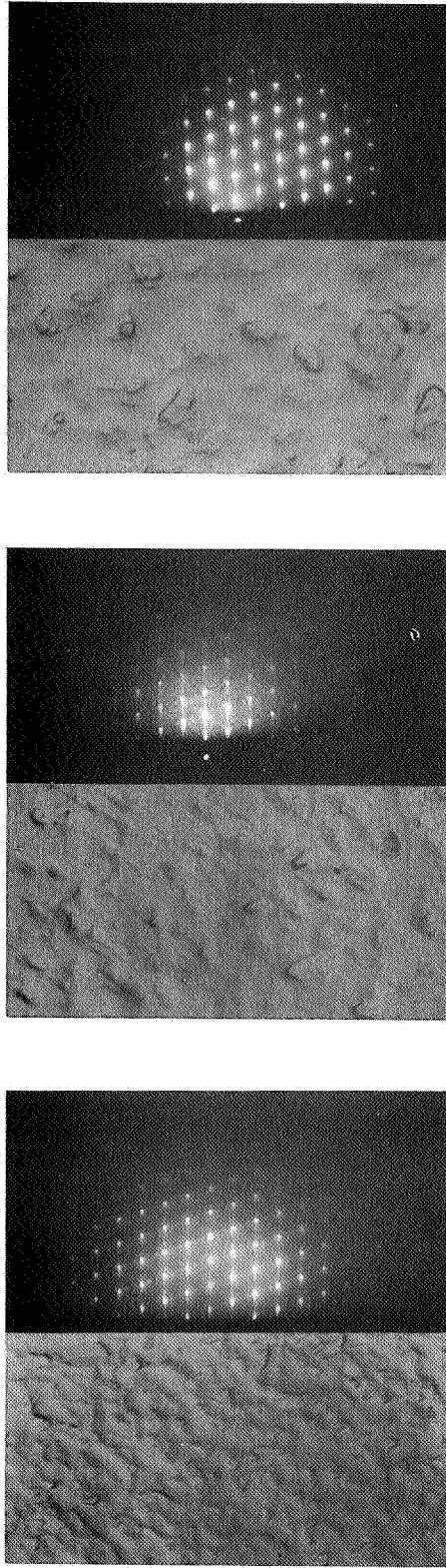


(c)



(d)

Figure 8. Replicas for (111) GaAs/(0001)  $Al_2O_3$  Films Grown at Setting of 250-45-0 at 675C for (a) 1 Sec; (b) 3 Sec; (c) 5 Sec; (d) 7 Sec (All Replicas at 20,000X)

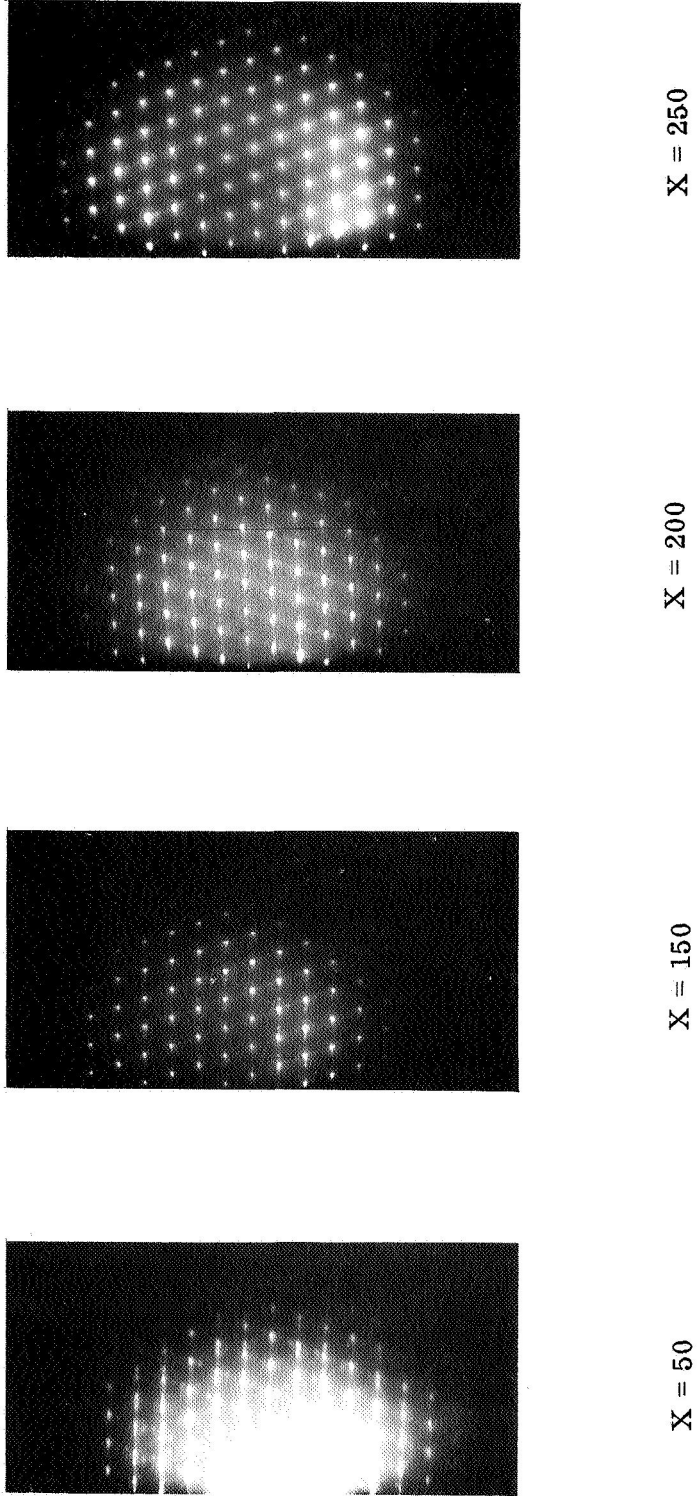


(a)

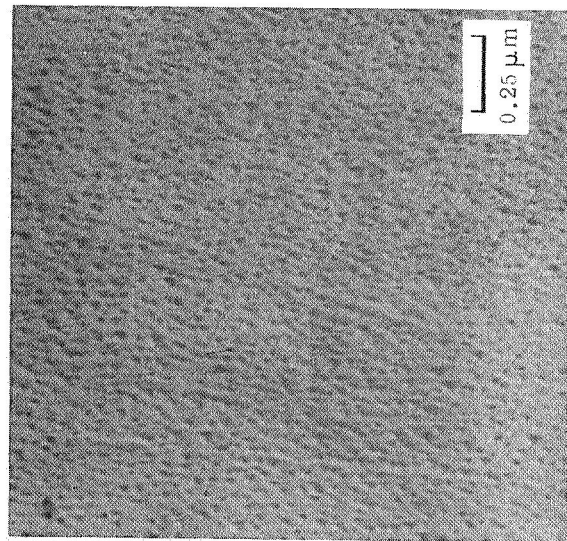
(b)

(c)

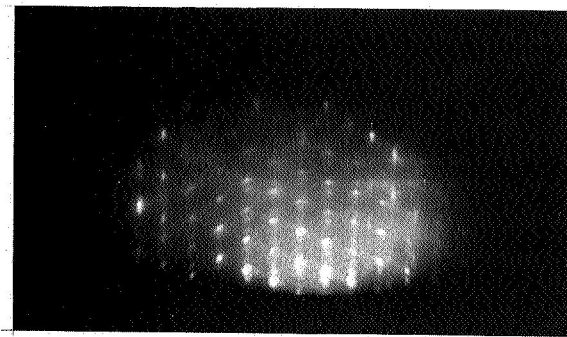
Figure 9. Replicas and (110) RED Patterns for (111) GaAs/(0001)Al<sub>2</sub>O<sub>3</sub> Films Grown at 675C at Setting of 200-45-0 for (a) 10 Sec; (b) 20 Sec; (c) 30 Sec (All Replicas at 20,000X)



(X-45-0)  
Figure 10.  $(110)$  XRD Patterns for  $(111)$  GaAs/ $(0001)$   $\text{Al}_2\text{O}_3$  Films Grown at  $675^\circ\text{C}$  for 1 Sec, for Different  $\text{AsH}_3$  Settings and Annealed at  $675^\circ\text{C}$  for 1 Hr



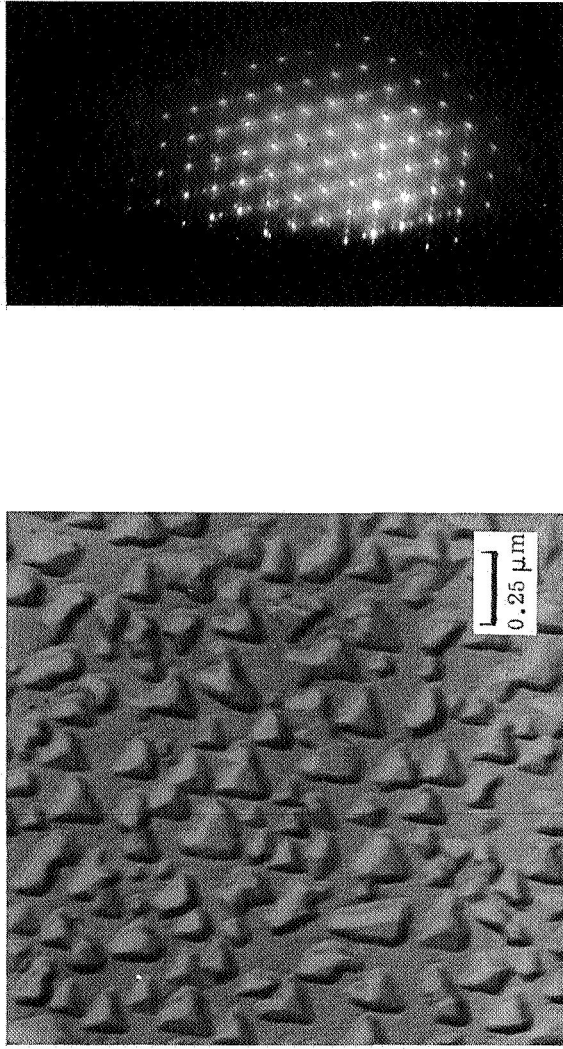
(a)



(b)

Figure 11. GaAs/(0001)  $\text{Al}_2\text{O}_3$  Produced by Reaction of Residual TMG with  $\text{AsH}_3$  for 1 Sec in an  $\text{AsH}_3$ - $\text{H}_2$  Atmosphere. a) Surface Structure at Magnification of 42,300X; b) (110) Reflection Electron Diffraction Pattern





(a)

(b)

Figure 12. GaAs/(0001) Al<sub>2</sub>O<sub>3</sub> Produced by Reaction of Residual TMG with AsH<sub>3</sub> for 6 Min in an AsH<sub>3</sub>-H<sub>2</sub> Atmosphere. a) Surface Structure at Magnification of 42, 300X; b) (110) Reflection Electron Diffraction Pattern

which suggest that twinned structures have formed. The RED patterns for these films indicate the presence of twins in the GaAs and also reveal some reflections due to the substrate material.

The high density of small island formation was also produced by decreasing the GaAs growth rate, i. e., by changing the TMG concentration. The differences in island density after 1 sec and 3 sec of growth may be observed in Figure 13 for two different growth rates and compared with Figure 8a for the 250-45-0 setting. Since the GaAs growth rate is directly proportional to the TMG flow rate, one finds the surface shown in Figure 8a (1 sec at TMG flowmeter setting of 45) to be intermediate to that of Figure 13d (3 sec at TMG flowmeter setting of 20) and Figure 13b (3 sec at TMG flowmeter setting of 10).

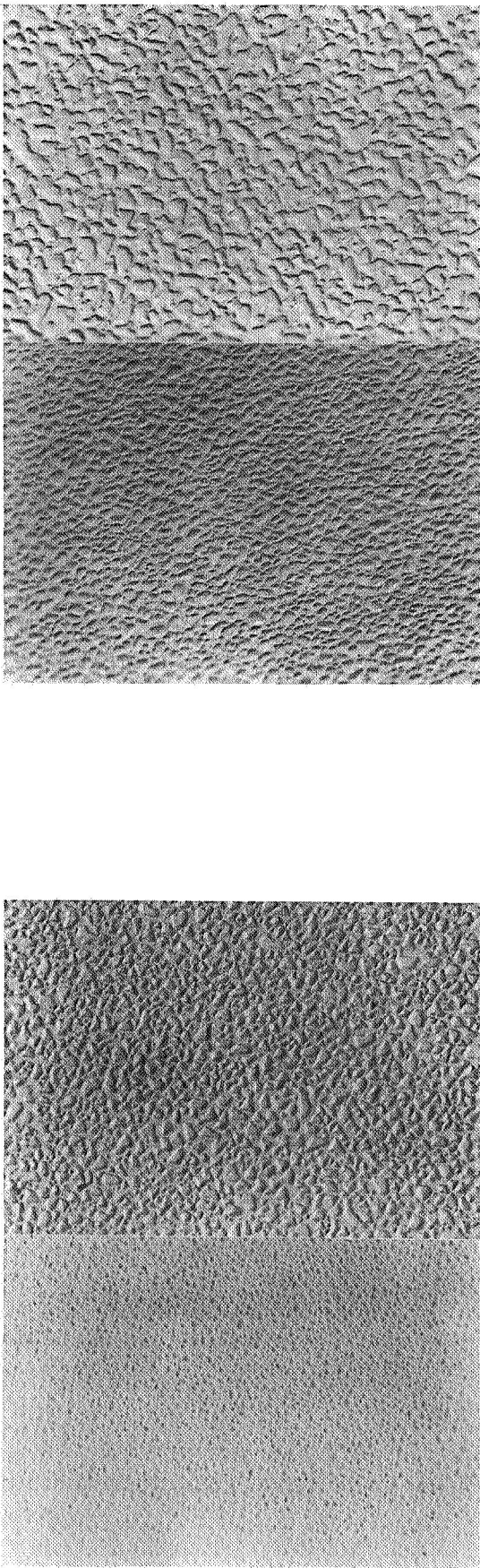
Replica electron microscopy and RED are also good tools for recording the effect of annealing on these very thin films. As shown in Figure 14, annealing a 1 sec-film growth for 1 hour at 600C and 675C caused the coalescence of the GaAs islands to molten-like masses, which occasionally exhibited an "epitaxial" order. Annealing of a 3-sec-growth film (Figure 15) produced larger islands of GaAs, mostly joined in a random-like fashion. Annealing of a 3-sec growth made under poor growth conditions (deficient in AsH<sub>3</sub>) yielded a structure which produced a RED pattern with multiple diffraction spots (Figure 16), indicative of the poor film quality.

Although the Al<sub>2</sub>O<sub>3</sub> surface appeared to be completely covered with GaAs after 5 sec (Figure 17) and 7 sec of growth (Figure 18), annealing at 600C and 675C revealed the presence of "islands" of bare Al<sub>2</sub>O<sub>3</sub>. The formation of islands was not attributed to volatilization of material at impurities on the surface but to coalescence, since most of the replicas appear to show that, once formed, only the number of islands is changing, not the total amount of exposed Al<sub>2</sub>O<sub>3</sub>. No islands were observed after annealing a 10-sec growth of GaAs (0.15μm thick) up to temperatures of 725C (Figure 19). Although some changes in film topography were observed, the RED pattern revealed twin structures at the film surface. As already shown in Figure 9(b, c), the twin structure is not evident in the RED patterns for the 20-sec and 30-sec growths. However, some variation in surface structure is apparent. Annealing a 30-sec growth at 725C for 1 hour (Figure 20) produced a relatively smooth film, possessing a terraced, plateau-like structure. The RED pattern appeared to be better than that of the unannealed film and closely resembled that of bulk GaAs.

These data indicate that further studies of the effect of changes of deposition parameters on the growth of thin films (1500Å or less) are necessary in order to attempt to improve the quality of GaAs heteroepitaxial films on Al<sub>2</sub>O<sub>3</sub>. When the conditions are established for the growth of "10-sec" films free from twinning, the quality of the heteroepitaxial composite must improve. It is expected that such growth conditions will also be applicable to improving GaAs homoepitaxial growth.

Effects of heat treatment on electrical properties. -- Preliminary studies of the effects of heat treatment on the electrical properties of GaAs/Al<sub>2</sub>O<sub>3</sub> films have also been undertaken.

Thick samples. -- A series of annealing experiments on a group of three relatively thick GaAs/Al<sub>2</sub>O<sub>3</sub> samples has been carried out. The pertinent electrical



(a)  
1 sec

(b)  
3 sec

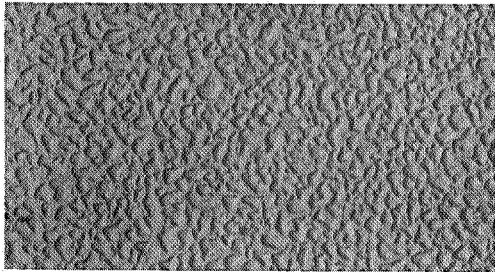
(c)  
1 sec

(d)  
3 sec

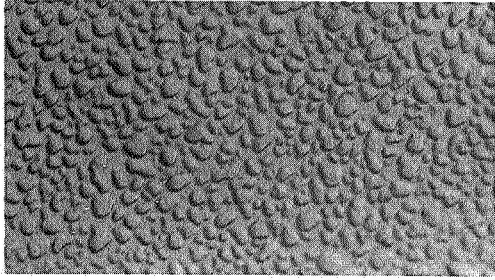
250-10-0

250-20-0

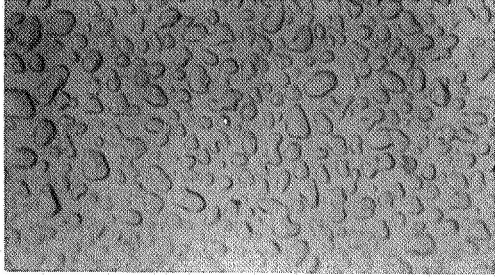
Figure 13. Replicas for (111) GaAs/(0001)  $Al_2O_3$  Films Grown at 675C for Different TMG Settings and Times. a) At 250-10-0 for 1 Sec; b) At 250-10-0 for 3 Sec; c) At 250-20-0 for 1 Sec; d) At 250-20-0 for 3 Sec. (All Replicas at 20,000X)



(a)

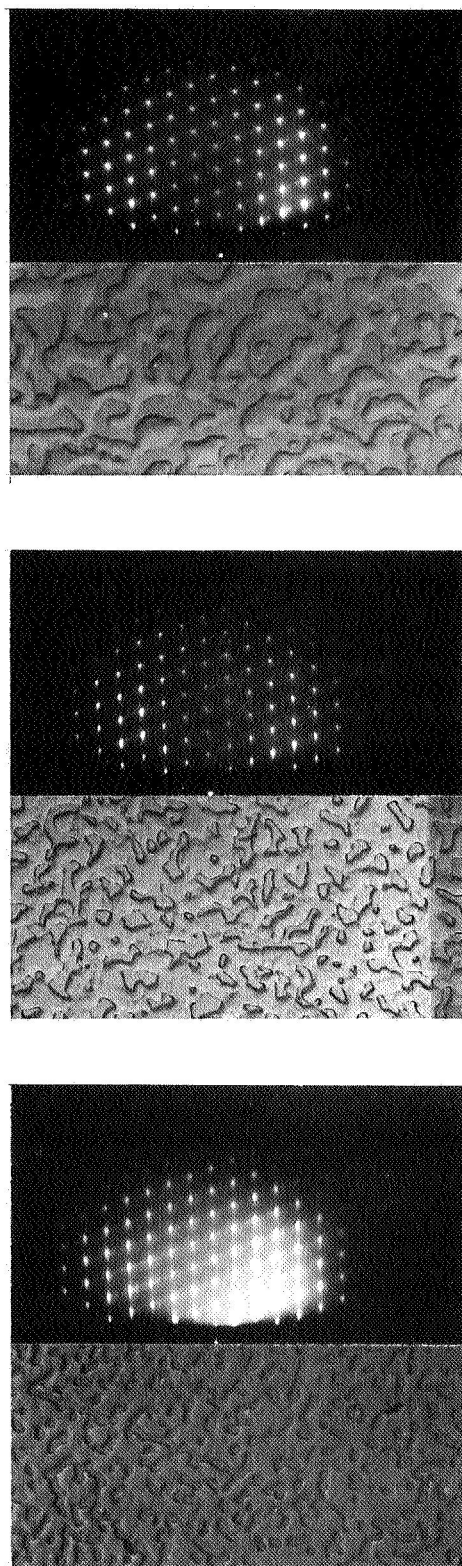


(b)



(c)

Figure 14. Replicas for (111) GaAs/(0001)  $Al_2O_3$  Films Grown for 1 Sec at Setting of 250-45-0. a) As Grown; b) After Annealing in  $AsH_3$  for 1 Hr at 600C; c) After Annealing in  $AsH_3$  for 1 Hr at 675C. (All Replicas at 20,000X)

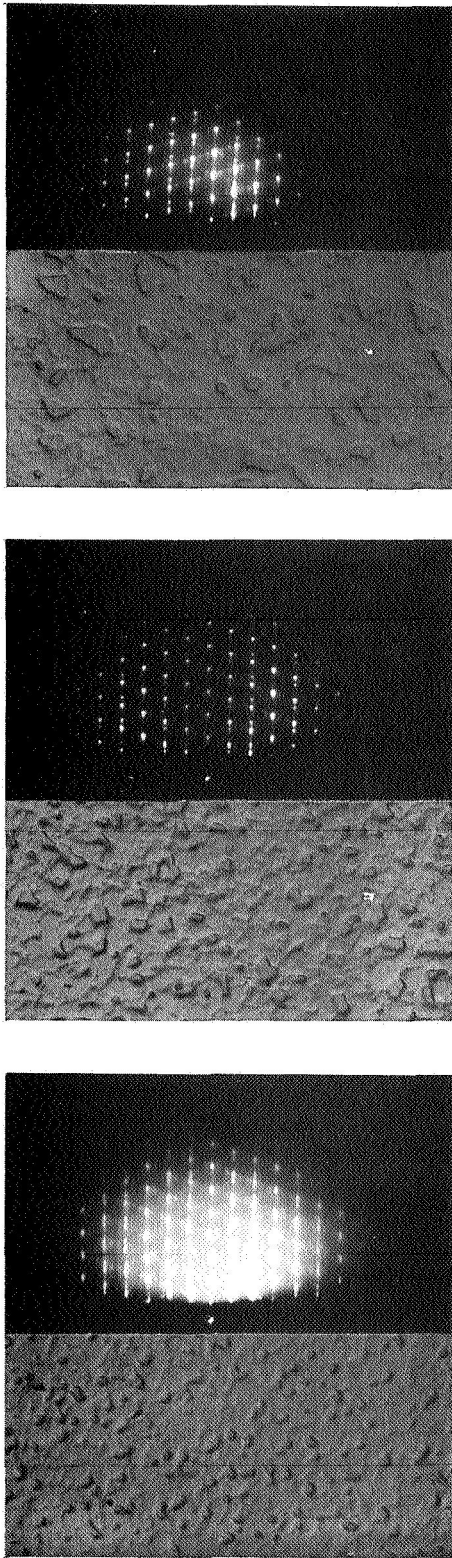


(a)

(b)

(c)

Figure 15. Replicas and RED Patterns for a GaAs/(0001)  $Al_2O_3$  Film Grown for 3 Seconds at Setting of 250-45-0. (a) As Grown; (b) After Annealing in  $AsH_3$  for 1 Hr at 600C; (c) After Annealing in  $AsH_3$  for 1 Hr at 675C. (All Replicas at 20,000X)

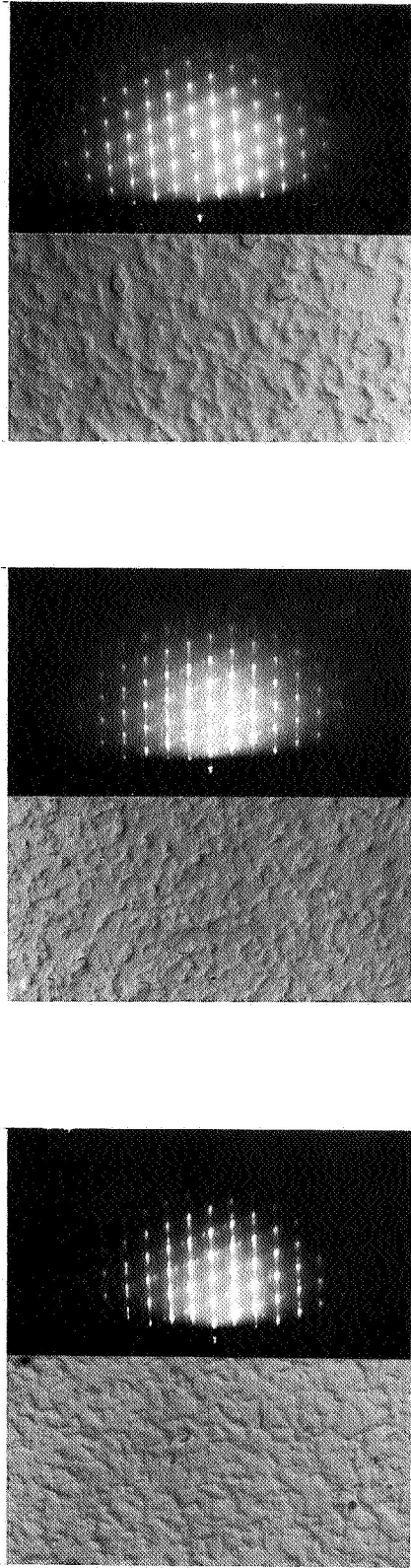


(a)

(b)

(c)

Figure 16. Replicas and RED Patterns for a GaAs/(0001)  $\text{Al}_2\text{O}_3$  Film Grown for 3 Seconds at Setting of 50-45-0. (a) As Grown; (b) After Annealing in  $\text{AsH}_3$  for 1 Hr at 600C; (c) After Annealing in  $\text{AsH}_3$  for 1 Hr at 675C (All Replicas at 20,000X)

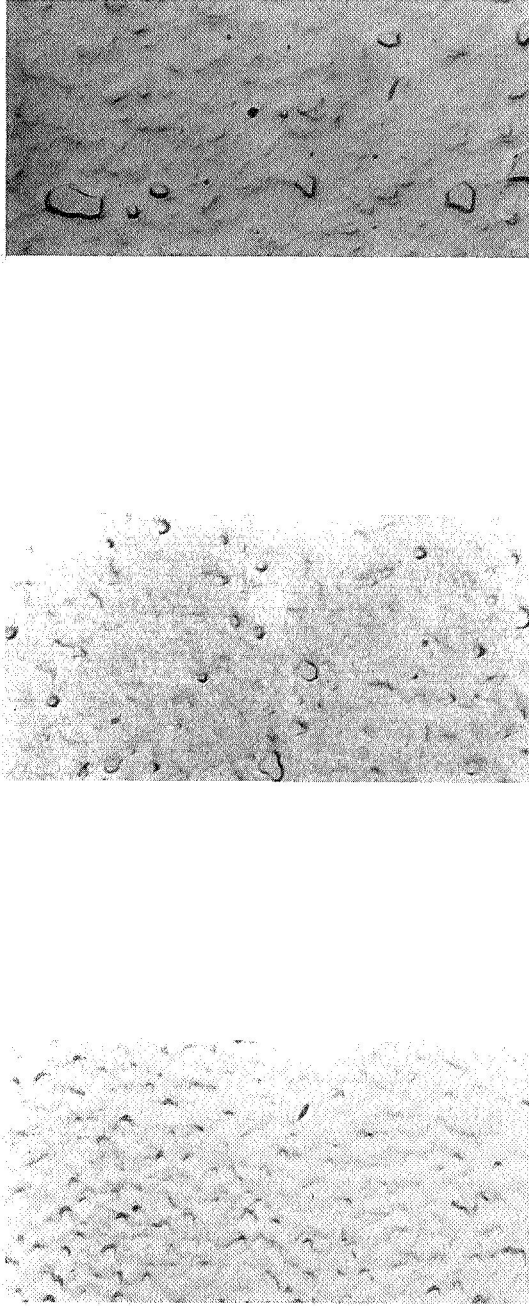


(a)

(b)

(c)

Figure 17. Replicas and (110) RED Patterns for (111) GaAs/(0001)  $\text{Al}_2\text{O}_3$  Films Grown for 5 Seconds at Setting of 250-45-0; a) As Grown; b) After Annealing in  $\text{AsH}_3$  for 1 Hr at 600C; c) After Annealing in  $\text{AsH}_3$  for 1 Hr at 675C. (All Replicas at 20, 000X)



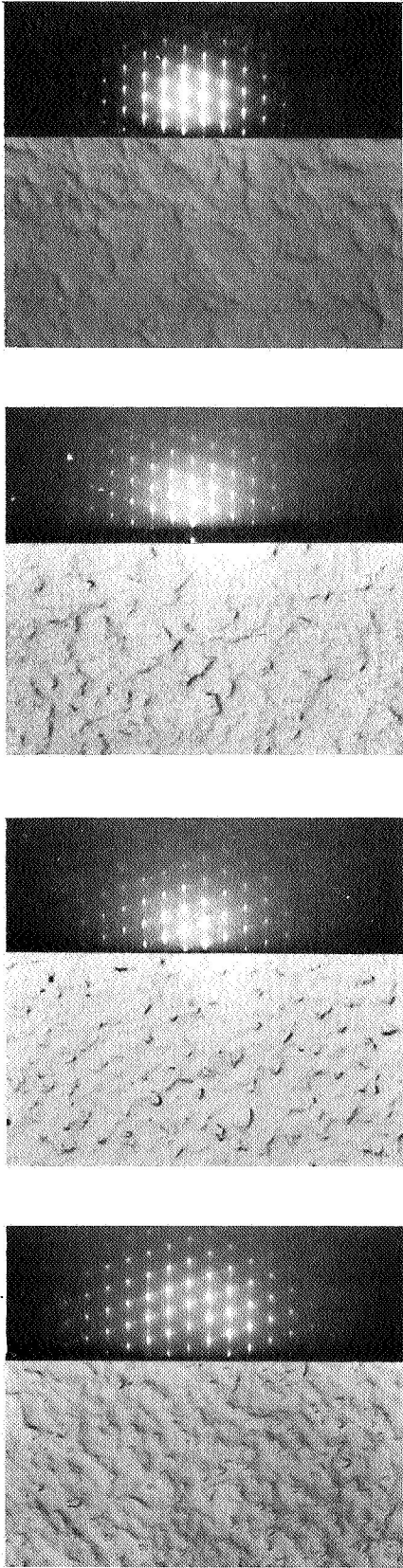
(a)

(b)

(c)

Figure 18. Replicas for (111) GaAs/(0001) Al<sub>2</sub>O<sub>3</sub> Films Grown for 7 Sec at Setting of 250-45-0. a) As Grown; b) After Annealing in AsH<sub>3</sub> for 1 Hr at 600C; c) After Annealing in AsH<sub>3</sub> for 1 Hr at 675C. (All Replicas at 20, 000X)





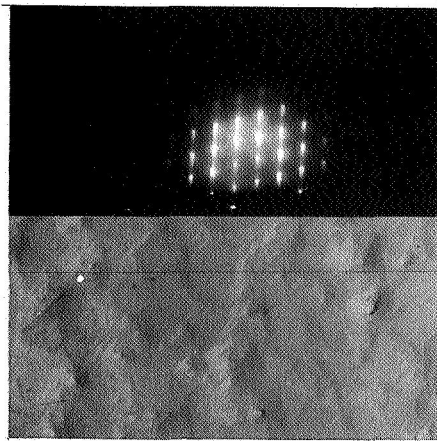
(a)

(b)

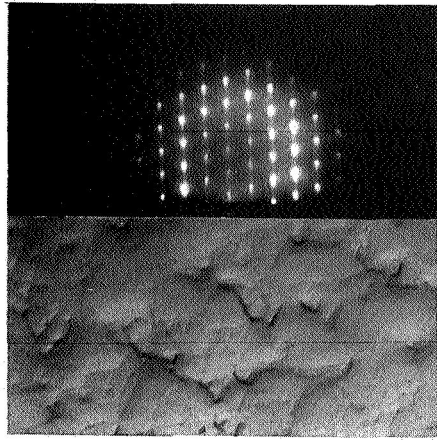
(c)

(d)

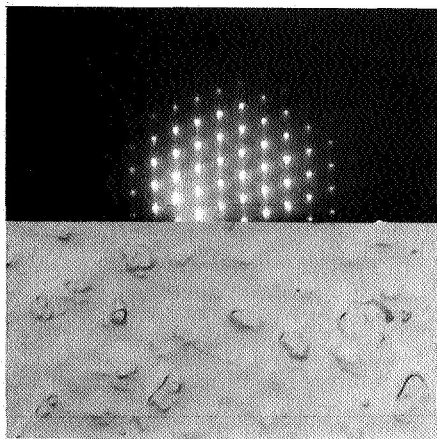
Figure 19. Replicas and (110) RED Patterns for (111) GaAs/(0001)  $Al_2O_3$  Films Grown for 10 Sec at Setting of 250-45-0. a) As Grown; b) After Annealing in  $AsH_3$  for 1 Hr at 600C; c) After Annealing in  $AsH_3$  for 1 Hr at 675C; d) After Annealing in  $AsH_3$  for 1 Hr at 725C. (All Replicas at 20,000X)



(a)



(b)



(c)

Figure 20. Replicas for (110) RED Patterns for (111) GaAs/(0001)  $Al_2O_3$  Films Grown for 30 Sec at Setting of 250-45-0. a) As Grown; b) After Annealing in  $AsH_3$  for 1 Hr at 675C; c) After Annealing in  $AsH_3$  for 1 Hr at 725C. (All Replicas at 20, 000X)

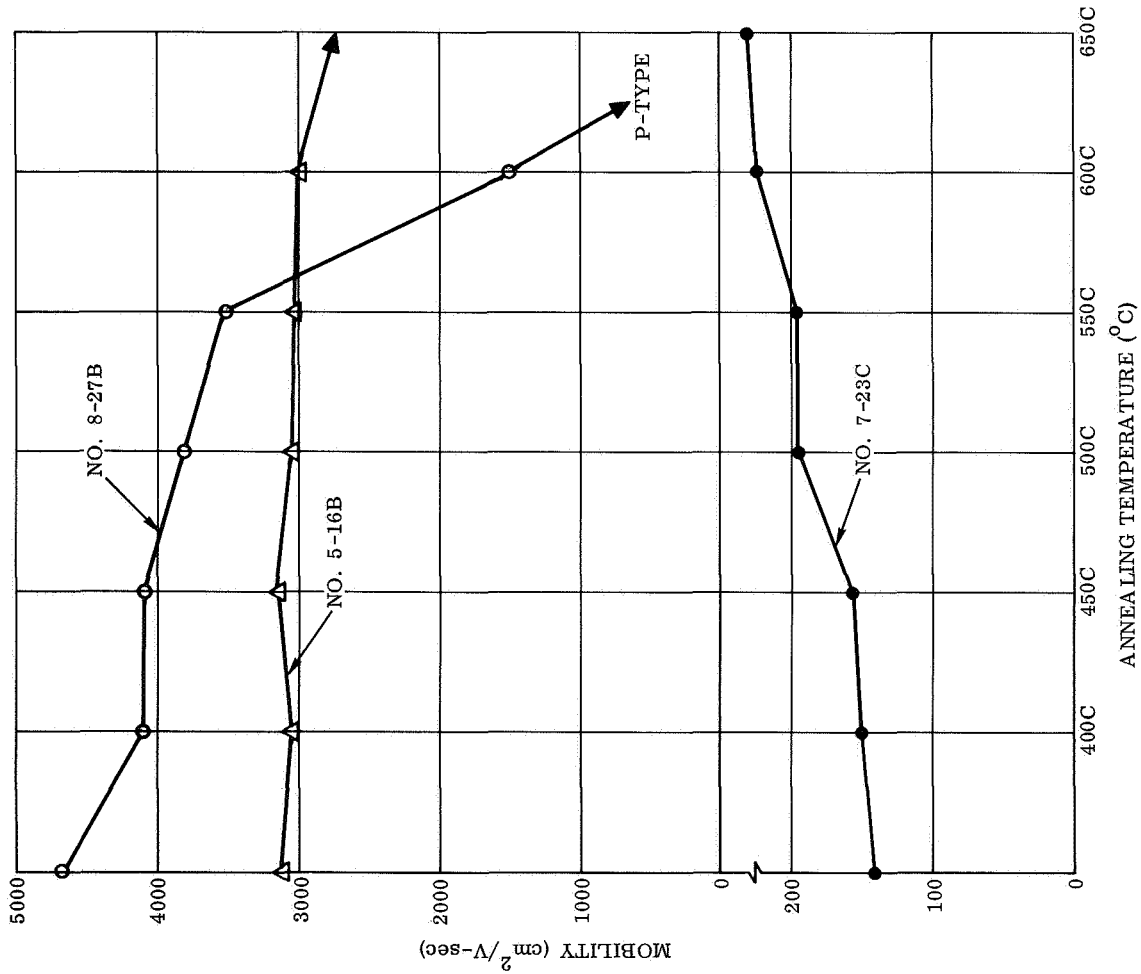
data on the as-grown samples are shown in Figure 21. The samples were successively measured and annealed in a flowing  $H_2 - AsH_3$  mixture at various temperatures for one hour (shown as the abscissa in the figure). The average mobility after the anneal at a given temperature is shown plotted as the ordinate at that temperature. It can be seen from the figure that the mobility of the Se-doped sample (#5-16B) changed very little with annealing up to 650C. Similarly, the carrier concentration was found to decrease by only 13 percent. The undoped sample (#8-27B) experienced a continuing decrease in mobility which became very pronounced after the 550C anneal. The carrier concentration at the same time dropped from  $\sim 1 \times 10^{16}$  to  $5 \times 10^{15} \text{ cm}^{-3}$ . After the 650C anneal this sample converted to p-type with an acceptor carrier concentration of  $\sim 10^{16} \text{ cm}^{-3}$  and a mobility of  $290 \text{ cm}^2/\text{V-sec}$ . The p-type sample for the same annealing sequence changed only slightly; the mobility increased from 140 to  $230 \text{ cm}^2/\text{V-sec}$ , and the carrier concentration decreased from  $3 \times 10^{16}$  to  $2 \times 10^{16} \text{ cm}^{-3}$ .

Thin samples. -- Preliminary investigation of the behavior of thin p-type (undoped) GaAs/ $Al_2O_3$  samples have been undertaken during the later part of the program. A group of  $1 \mu\text{m}$ -thick samples was grown under identical growth conditions except for annealing steps during or after growth. Unannealed samples grown as controls were found to have p-type carrier concentrations from  $2 \times 10^{16}$  to  $2 \times 10^{17} \text{ cm}^{-3}$ . For a similar sample annealed at a temperature from 600 to 720C for one hour after growth, the carrier concentrations became quite small, from  $10^{12}$  to  $10^{14} \text{ cm}^{-3}$ . If the annealing is done just after the film has nucleated (after, say,  $1500 \text{ \AA}$  of growth) and growth is then continued to a thickness of  $1 \mu\text{m}$ , the carrier concentration remains in the  $10^{16}$  to  $10^{17} \text{ cm}^{-3}$  range.

It is apparent from these examples that a one hour anneal at or near the growth temperature after  $1 \mu\text{m}$  of film growth has a profound effect on the electrical properties of the thin films. Although the electrical data are not definitive at this point, there is a trend for the annealed samples to have a slightly higher mobility than those that are not annealed. This result would tend to be consistent with the improvement in crystal structure observed after anneal of very thin films, as discussed in the section on nucleation studies.

The mechanism that produces these effects is at present unknown. It is interesting to note, however, that the same annealing experiments on  $5 \mu\text{m}$  p-type films do not produce a decrease in carrier concentration. Such behavior may be related to the decreasing concentration of defects as the distance from the interface increases. On the other hand a compensating impurity on the  $Al_2O_3$  substrate might produce the above results if it could diffuse into the film during anneal. Since the annealing temperatures are quite low, diffusion might not be expected to take place (except perhaps for some fast diffusers like Cu) were it not for the fact that the high defect structure near the interface could well enhance the diffusion process over that which occurs in normal bulk material. This mechanism might explain the quite different results between the  $1 \mu\text{m}$  and  $5 \mu\text{m}$  films.

With regard to the growth of thin films, electrical measurements on several films grown subsequent to the above have shown that the high p-type concentrations are not consistently found in  $1 \mu\text{m}$  films. Several unannealed samples grown by the same process (with identical growth conditions) were found to have hole concentrations ranging from  $\sim 10^{12}$  to  $>10^{15} \text{ cm}^{-3}$ . Recent undoped unannealed films  $1 \mu\text{m}$  thick grown in the He system were found to have resistivities  $>10^5 \text{ ohm-cm}$ . Since it is desirable to minimize (or eliminate) the p-type behavior at the interface, the



ORIGINAL CHARACTERISTICS

#8-27B:  $n = 1.2 \times 10^{16} \text{ cm}^{-3}$

$\rho = 0.11 \Omega\text{-cm}$

$\mu = 4650 \text{ cm}^2/\text{V-sec}$

GROWN UNDOPED @ 660C  
THICKNESS = 15.4  $\mu\text{m}$

#5-16B:  $n = 1.7 \times 10^{17} \text{ cm}^{-3}$

$\rho = 0.012 \Omega\text{-cm}$

$\mu = 3100 \text{ cm}^2/\text{V-sec}$

SE DOPED DURING GROWTH AT 700C  
THICKNESS = 9.4  $\mu\text{m}$

#7-23C:  $n = 3.4 \times 10^{16} \text{ cm}^{-3}$

$\rho = 1.3 \Omega\text{-cm}$

$\mu = 140 \text{ cm}^2/\text{V-sec}$

GROWN P-TYPE BY REDUCTION  
OF  $\text{AsH}_3$  FLOW DURING GROWTH AT 675C  
THICKNESS = 39  $\mu\text{m}$

Figure 21. Effect of Annealing on the Mobility of Three GaAs/Al<sub>2</sub>O<sub>3</sub> Films

causes of the variations in the acceptor concentrations discussed above are of paramount importance. At present there appears to be no correlation between the growth conditions and the resulting acceptor concentration.

Growth of GaAs on spinel. -- The high defect structure possessed by commercial-type Verneuil spinel is readily revealed by the epitaxial growth of GaAs, as shown in Figure 22. However, good quality (111) Czochralski spinel has been a good substrate for GaAs growth; simultaneous growth on (111)  $MgAl_2O_4$  and (0001)  $Al_2O_3$  has produced epitaxial films of equivalent high quality. The apparent advantage to the use of spinel as a substrate lies in its cubic structure, thereby making it a possible insulating substrate for the growth of practically any orientation of the zinc-blende materials, represented in this case by GaAs. The GaAs/ $Al_2O_3$  orientation studies have not established a substrate orientation for (100) GaAs growth; consequently, a boule of commercially available Czochralski spinel was oriented to the (100), sliced into wafers, and mechanically polished. (100) GaAs was grown on the wafers, but good growth conditions were not reproducible. X-ray topography (see Figure 23) revealed strain in the crystal and optical microscopy showed scratches on the surface. Additional polishing to remove the scratches was performed at Autonetics, but only partial success was achieved, as revealed by the GaAs overgrowth. The reflectivity of the (100) GaAs/(100)  $MgAl_2O_4$  composite is shown in Figure 24; the surface structure is shown in Figure 25. The epitaxy indicates that variations in quality exist within the substrate.

Growth of GaAs on ruby. -- Simultaneous GaAs growth at 675C on (0001)  $Al_2O_3$  and Cr-doped (0001)  $Al_2O_3$  produced films with essentially equivalent electrical and physical characteristics. Annealing these films for at least 1 hour at 725C did not electrically affect p-type films  $1\mu m$  thick. From this, it appears that autodoping due to Cr at the usual growth temperatures for GaAs is not an important consideration at the GaAs- $Al_2O_3$  interface. If Cr had diffused through the interface, a conversion to higher resistivity GaAs might have been expected.

Doping studies with diethylzinc. -- Prior to the initiation of the contract some Zn-doped samples had been grown, and a set of conditions was established for the growth of films with a wide range of p-type carrier concentrations. During the contract period a new apparatus was constructed, and a study was begun to relate different growth parameters to the quality of the Zn-doped GaAs. Preliminary results indicating the effect of some of these variables are shown in Figure 26, in which hole concentration p is plotted versus  $H_2$  flow rate over DEZ. The solid dots show the variation in p at 725C. The crosses illustrate the variation in p at 700C with a fixed Zn impurity concentration (i. e., constant flow rate of  $H_2$  over DEZ) and a fixed  $AsH_3$  flow rate, but with changes in TMG rate and hence in growth rate. In both cases the limits of doping have been  $\sim 3 \times 10^{19} cm^{-3}$ . The p-type doping level is found to be quite dependent on the TMG concentration. The Hall mobilities of these p<sup>+</sup> films have been in the range from 50-100  $cm^2/V$ -sec with corresponding resistivities  $\sim 0.003$ - $0.01$  ohm-cm.

The doping of GaAs films with DEZ has also been demonstrated using He in place of  $H_2$  in the gas supplies. The solubility limit of Zn and the role of He, if any, in determining this limit have not yet been established for GaAs layers grown in the inert atmosphere.

Orientation relationships. -- X-ray diffraction and reflection electron diffraction techniques are being used to determine the crystallographic relationships between epitaxial GaAs and  $Al_2O_3$ , as was performed in the Si-on- $Al_2O_3$  system (Ref. 6). The  $Al_2O_3$  substrate orientations being studied are indicated in a portion of the  $Al_2O_3$



Figure 22. The Effect of Grain Boundaries in the Verneuil Spinel on the Growth of GaAs

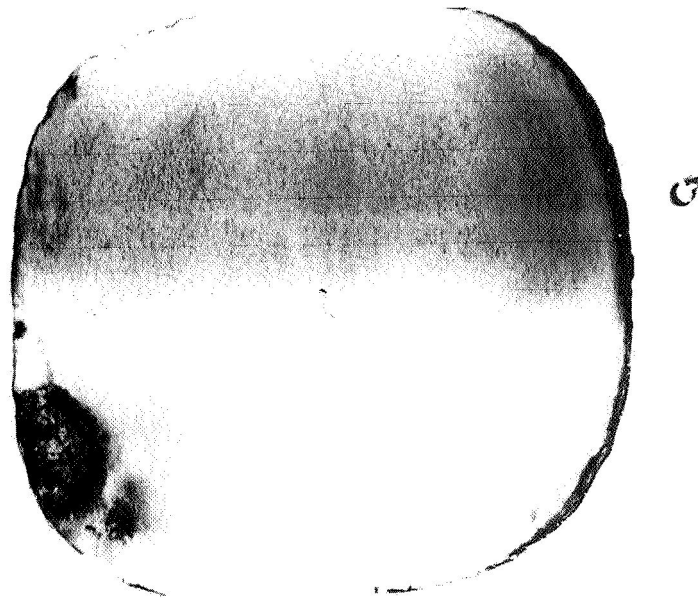


Figure 23. A Lang X-ray Topograph of (100) Czoehralski Spinel Revealing Strained Areas (Dark Portions) in the Crystal (about 0.5 in. square)

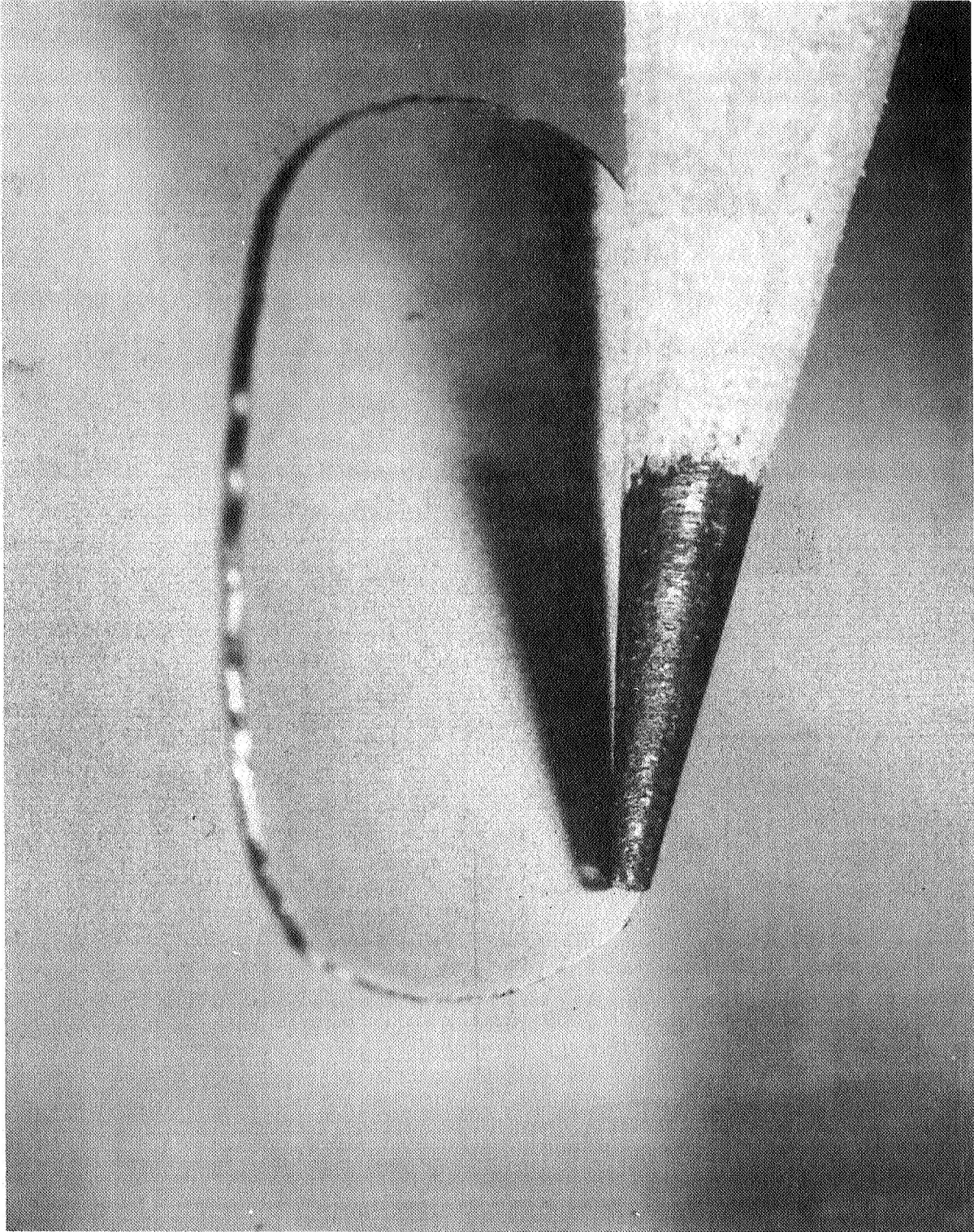


Figure 24. Reflectivity of (100) GaAs Growth on a 0.5-Inch Wide (100) Spinel Substrate

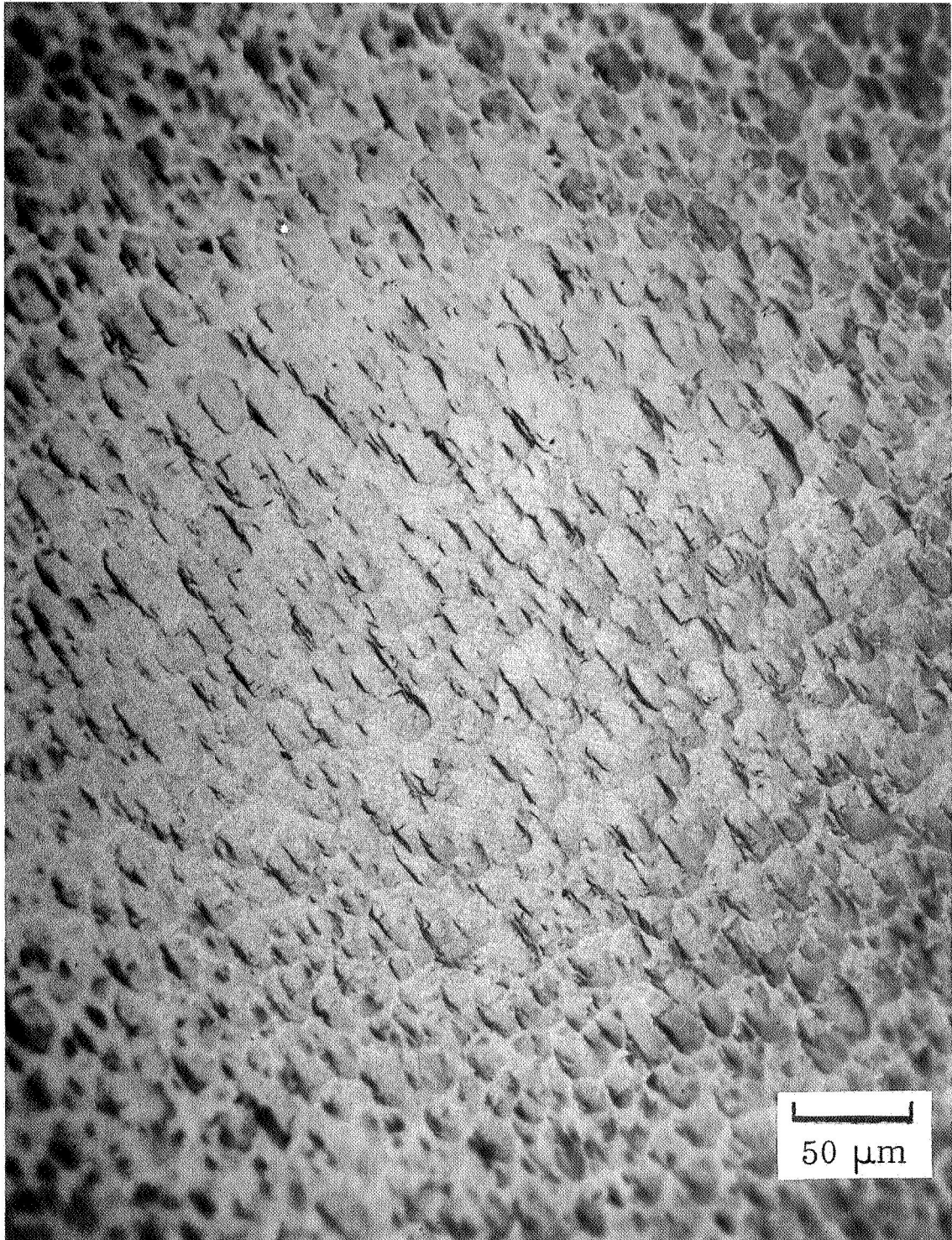


Figure 25. Surface Structure of (100) GaAs Growth on (100) Spinel



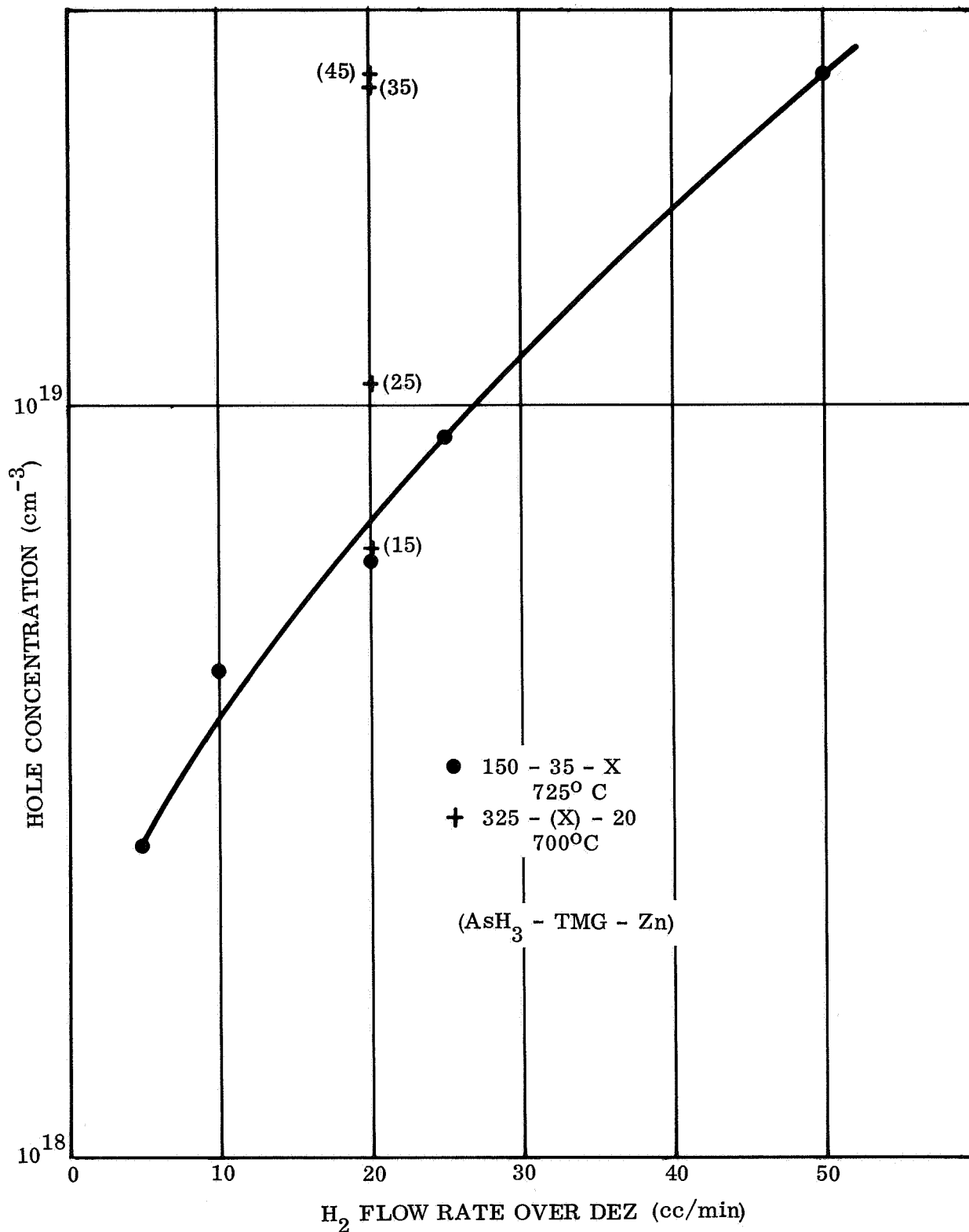


Figure 26. Hole Concentration in (111) GaAs Films Grown on (0001) Al<sub>2</sub>O<sub>3</sub> as a Function of Diethylzinc (DEZ) and Trimethylgallium (TMG) Concentration

stereographic projection, as in Figure 27. These orientations lie primarily along six principal zones:

- A.  $(0001) Al_2O_3 \rightarrow (10\bar{1}4) Al_2O_3$
- B.  $(10\bar{1}4) Al_2O_3 \rightarrow (01\bar{1}5) Al_2O_3$
- C.  $(10\bar{1}1) Al_2O_3 \rightarrow (12\bar{3}2) Al_2O_3$
- F.  $(01\bar{1}2) Al_2O_3 \rightarrow (11\bar{2}3) Al_2O_3$
- I.  $(11\bar{2}0) Al_2O_3 \rightarrow (0001) Al_2O_3$
- J.  $(12\bar{3}2) Al_2O_3 \rightarrow (01\bar{1}2) Al_2O_3$

The growth of the GaAs films on the above orientations was performed using essentially those deposition conditions which have been sufficient for GaAs growth on  $(0001) Al_2O_3$ . The major change sometimes required was temperature, some orientations appearing to grow better at 750C than at 675C.

The specific substrate orientations and the heteroepitaxial relationships found to date for the GaAs/ $Al_2O_3$  system are summarized in Table XI.

Good deposits have been obtained on basal plane, i. e.,  $(0001)$ -oriented, substrates. The relationships obtained are  $(111) GaAs \parallel (0001) Al_2O_3$  with  $[01\bar{1}] GaAs \parallel [12\bar{1}0] Al_2O_3$ . On analyzing the  $Al_2O_3$  planes A1 and A3 (see Figure 27) on the zone between the  $(0001)$  and the  $(10\bar{1}4)$  planes of  $Al_2O_3$ , the predominant orientation was found to be the  $(111) GaAs$  plane parallel to the  $(0001)$  face of the  $Al_2O_3$  substrate. However, a  $(111) GaAs$  reflection was also found parallel to the  $(10\bar{1}4) Al_2O_3$  reflection. These two  $\{111\}$  GaAs planes are twins. On A2, substrate plane cut 19 deg from the basal plane of  $Al_2O_3$ , the  $(111)$  plane of GaAs is not parallel to  $(0001) Al_2O_3$  but tilted 5 deg from it. Analysis of a deposit on  $(10\bar{1}4) Al_2O_3$  indicates the presence of  $(111) GaAs$ , but of poor quality.

Reflective deposits have been formed on two substrates (B1 and B2) that lie 18 and 25 deg from the  $(10\bar{1}4)$  plane on the zone toward  $(01\bar{1}5) Al_2O_3$ . On both of the substrates the following relations were detected:  $(111) GaAs$  nearly parallel to  $(0001) Al_2O_3$ ;  $(111) GaAs$  nearly parallel to  $(10\bar{1}4) Al_2O_3$ ; and the  $(110) GaAs \parallel (01\bar{1}8) Al_2O_3$ , which is consistent with  $(111) GaAs \parallel (10\bar{1}4) Al_2O_3$ . The results also imply a twin relationship between the two  $(111) GaAs$  growths on  $(0001)$  and  $(10\bar{1}4) Al_2O_3$ , and a consistency with the analyses of the films grown on the A1, A2, and A3 substrates.

On substrates C1 to C5, cut along the zone between the  $(10\bar{1}1)$  and the  $(12\bar{3}2)$  planes of  $Al_2O_3$ , it was found that a pole representing  $(111) GaAs$  was consistently near the  $(11\bar{2}3) Al_2O_3$ , despite the wide spread in angular relationships ( $\sim 40$  deg) of the five (C1 to C5) substrates. However, the  $(111) GaAs$  plane was found to be tilted from the substrate, the degree of tilt increasing from 3 to 5 deg as the substrate orientation approached the  $(12\bar{3}2)$  plane of  $Al_2O_3$ . Analyses on C3 and C4 show that the pole representing the  $(111) GaAs$  lies about 5 deg from the  $(11\bar{2}3)$  pole of  $Al_2O_3$  toward the  $(11\bar{2}0)$  pole of  $Al_2O_3$ . At the same time, the  $(111)$  twin plane of GaAs falls about 5 deg from the  $(11\bar{2}0)$  pole of  $Al_2O_3$ .

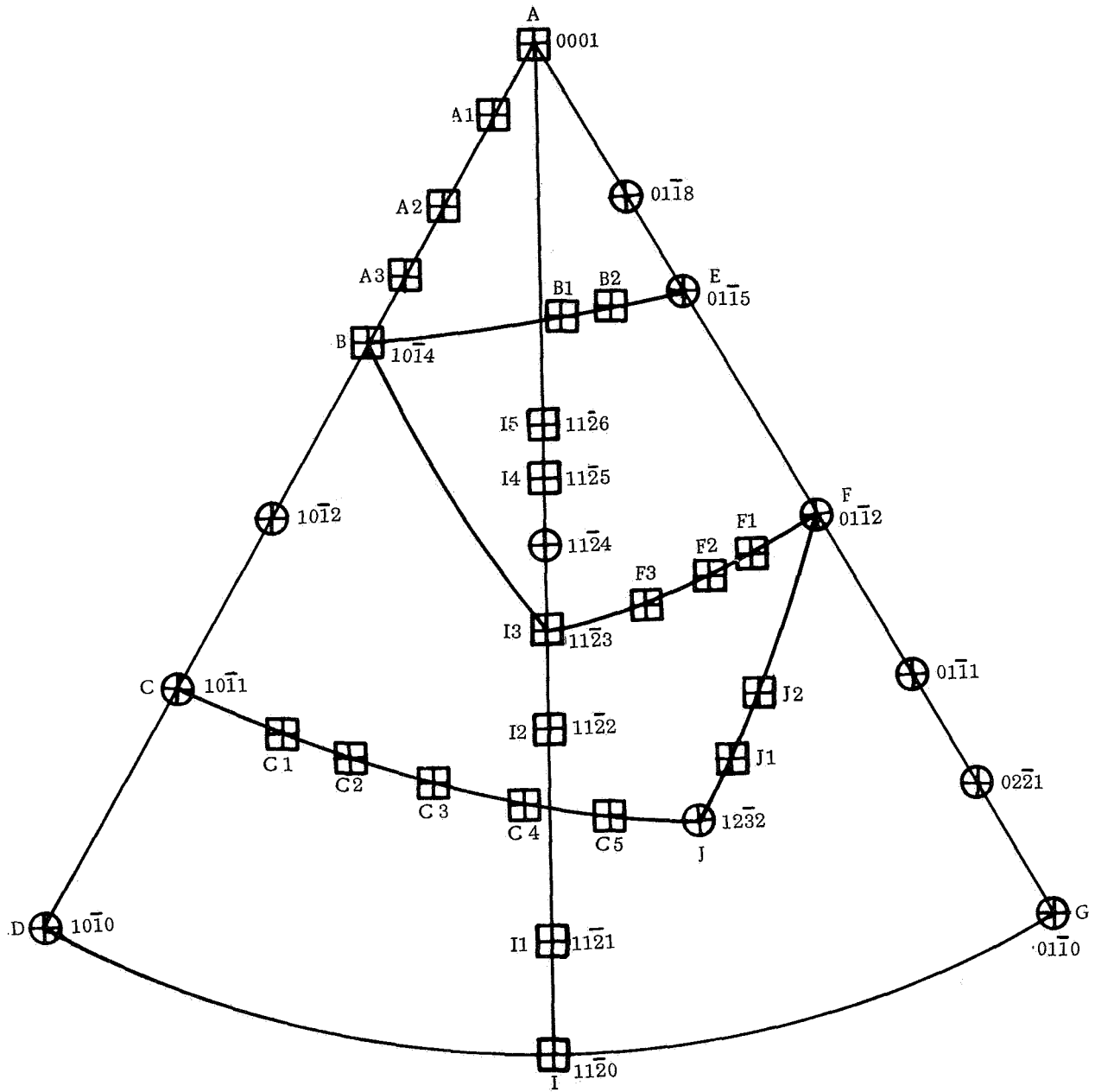



Figure 27. Portion of a Stereographic Projection of  $Al_2O_3$ . The symbol  Indicates Orientations Investigated.

TABLE XI. GaAs/Al<sub>2</sub>O<sub>3</sub> CRYSTALLOGRAPHIC RELATIONSHIPS FROM X-RAY DIFFRACTION STUDIES

Zone	Substrate		Orientation	
	Designation	Orientation	Planes	Direction
(0001) Al <sub>2</sub> O <sub>3</sub>	A	(0001)	(111) GaAs // (0001) Al <sub>2</sub> O <sub>3</sub>	[01 $\bar{1}$ ] GaAs // [ $\bar{1}2\bar{1}0$ ] Al <sub>2</sub> O <sub>3</sub>
to	A1	9° from (0001) toward (10 $\bar{1}4$ )	(111) GaAs // (0001) Al <sub>2</sub> O <sub>3</sub> (111) GaAs // (10 $\bar{1}4$ ) Al <sub>2</sub> O <sub>3</sub>	[01 $\bar{1}$ ] GaAs // [ $\bar{1}2\bar{1}0$ ] Al <sub>2</sub> O <sub>3</sub>
(10 $\bar{1}4$ ) Al <sub>2</sub> O <sub>3</sub>	A2	19° from (0001) toward (10 $\bar{1}4$ )	(111) GaAs 5° from (0001) Al <sub>2</sub> O <sub>3</sub> (111) GaAs 5° from (10 $\bar{1}4$ ) Al <sub>2</sub> O <sub>3</sub>	[01 $\bar{1}$ ] GaAs 5° from [ $\bar{1}2\bar{1}0$ ] Al <sub>2</sub> O <sub>3</sub>
	A3	26° from (0001) toward (10 $\bar{1}4$ )	(111) GaAs // (0001) Al <sub>2</sub> O <sub>3</sub> (111) GaAs 5° from (10 $\bar{1}4$ ) Al <sub>2</sub> O <sub>3</sub>	[01 $\bar{1}$ ] GaAs // [ $\bar{1}2\bar{1}0$ ] Al <sub>2</sub> O <sub>3</sub>
(10 $\bar{1}4$ ) Al <sub>2</sub> O <sub>3</sub>	B	(10 $\bar{1}4$ )	(111) GaAs // (10 $\bar{1}4$ ) Al <sub>2</sub> O <sub>3</sub> of poor quality	--
to	B1	18° from (10 $\bar{1}4$ ) toward (01 $\bar{1}5$ )	(111) GaAs nearly // (0001) Al <sub>2</sub> O <sub>3</sub> (111) GaAs 5° from (10 $\bar{1}4$ ) Al <sub>2</sub> O <sub>3</sub>	[01 $\bar{1}$ ] GaAs // [ $\bar{1}2\bar{1}0$ ] Al <sub>2</sub> O <sub>3</sub> [01 $\bar{1}$ ] GaAs 5° from [ $\bar{1}2\bar{1}0$ ] Al <sub>2</sub> O <sub>3</sub>
(01 $\bar{1}5$ ) Al <sub>2</sub> O <sub>3</sub>	B2	25° from (10 $\bar{1}4$ ) toward (01 $\bar{1}5$ )	(111) GaAs nearly // (0001) Al <sub>2</sub> O <sub>3</sub> (111) GaAs 5° from (10 $\bar{1}4$ ) Al <sub>2</sub> O <sub>3</sub> (110) GaAs // (01 $\bar{1}8$ ) Al <sub>2</sub> O <sub>3</sub>	[01 $\bar{1}$ ] GaAs // [ $\bar{1}2\bar{1}0$ ] Al <sub>2</sub> O <sub>3</sub> [01 $\bar{1}$ ] GaAs 5° from [ $\bar{1}2\bar{1}0$ ] Al <sub>2</sub> O <sub>3</sub> [01 $\bar{1}$ ] GaAs // [ $\bar{1}100$ ] Al <sub>2</sub> O <sub>3</sub>
(10 $\bar{1}1$ ) Al <sub>2</sub> O <sub>3</sub>	C1	9.5° from (10 $\bar{1}1$ ) toward (12 $\bar{3}2$ )	(111) GaAs 3° from (11 $\bar{2}3$ ) Al <sub>2</sub> O <sub>3</sub>	[01 $\bar{1}$ ] GaAs // [01 $\bar{1}1$ ] Al <sub>2</sub> O <sub>3</sub>
to	C2	11.5° from (10 $\bar{1}1$ ) toward (12 $\bar{3}2$ )	(111) GaAs 3° from (11 $\bar{2}3$ ) Al <sub>2</sub> O <sub>3</sub>	[01 $\bar{1}$ ] GaAs // [01 $\bar{1}1$ ] Al <sub>2</sub> O <sub>3</sub>
(12 $\bar{3}2$ ) Al <sub>2</sub> O <sub>3</sub>				

TABLE XI (Continued)

Zone	Substrate		Orientation	
	Designation	Orientation	Planes	Direction
	C3	20° from (10 $\bar{1}$ 1) toward (12 $\bar{3}$ 2)	(111) GaAs 5° from (11 $\bar{2}$ 3) Al <sub>2</sub> O <sub>3</sub>	[01 $\bar{1}$ ] GaAs 6° from [1 $\bar{1}$ 00] Al <sub>2</sub> O <sub>3</sub>
	C4	25.5° from (10 $\bar{1}$ 1) toward (12 $\bar{3}$ 2)	(111) GaAs 5° from (11 $\bar{2}$ 3) Al <sub>2</sub> O <sub>3</sub>	[01 $\bar{1}$ ] GaAs // [1 $\bar{1}$ 00] Al <sub>2</sub> O <sub>3</sub>
	C5	34.5° from (10 $\bar{1}$ 1) toward (12 $\bar{3}$ 2)	(111) GaAs 5° from (11 $\bar{2}$ 3) Al <sub>2</sub> O <sub>3</sub>	[01 $\bar{1}$ ] GaAs // [1 $\bar{1}$ 00] Al <sub>2</sub> O <sub>3</sub>
	F	(01 $\bar{1}$ 2)	(111) GaAs // (01 $\bar{1}$ 2) Al <sub>2</sub> O <sub>3</sub>	[01 $\bar{1}$ ] GaAs // [2201] Al <sub>2</sub> O <sub>3</sub>
(01 $\bar{1}$ 2) Al <sub>2</sub> O <sub>3</sub>	F1	9° from (01 $\bar{1}$ 2) toward (11 $\bar{2}$ 3)	(110) GaAs // (01 $\bar{1}$ 2) Al <sub>2</sub> O <sub>3</sub>	[01 $\bar{1}$ ] GaAs // [0 $\bar{1}$ 11] Al <sub>2</sub> O <sub>3</sub>
to	F2	16° from (01 $\bar{1}$ 2) toward (11 $\bar{2}$ 3)	(111) GaAs 8° from (11 $\bar{2}$ 3) Al <sub>2</sub> O <sub>3</sub>	[01 $\bar{1}$ ] GaAs // [0 $\bar{1}$ 11] Al <sub>2</sub> O <sub>3</sub>
(11 $\bar{2}$ 3) Al <sub>2</sub> O <sub>3</sub>	F3	20° from (01 $\bar{1}$ 2) toward (11 $\bar{2}$ 3)	(111) GaAs 7.5° from (11 $\bar{2}$ 3) Al <sub>2</sub> O <sub>3</sub>	[01 $\bar{1}$ ] GaAs // [0 $\bar{1}$ 11] Al <sub>2</sub> O <sub>3</sub>

TABLE XI (Continued)

Zone	Substrate		Orientation	
	Designation	Orientation	Planes	Direction
(1120) Al <sub>2</sub> O <sub>3</sub> to (0001) Al <sub>2</sub> O <sub>3</sub>	I	(1120)	(111) GaAs 5° from (1120) to (1123) Al <sub>2</sub> O <sub>3</sub>	[011] GaAs // [1100] Al <sub>2</sub> O <sub>3</sub>
	I1	(1121)	(111) GaAs 10° from (1120) toward (1123) Al <sub>2</sub> O <sub>3</sub>	[011] GaAs // [1100] Al <sub>2</sub> O <sub>3</sub>
	I2	(1122)	(311) GaAs // (1122) Al <sub>2</sub> O <sub>3</sub> with (111) GaAs // (1123) Al <sub>2</sub> O <sub>3</sub>	[011] GaAs // [1100] Al <sub>2</sub> O <sub>3</sub>
	I3	(1123)	(111) GaAs // (1123) Al <sub>2</sub> O <sub>3</sub>	[011] GaAs // [1100] Al <sub>2</sub> O <sub>3</sub>
	I4	(1125)	(111) GaAs // (1125) Al <sub>2</sub> O <sub>3</sub>	[011] GaAs // [1100] Al <sub>2</sub> O <sub>3</sub>
	I5	(1126)	(111) GaAs // (1126) Al <sub>2</sub> O <sub>3</sub> (211) GaAs 2° from (1014) Al <sub>2</sub> O <sub>3</sub>	[011] GaAs // [1100] Al <sub>2</sub> O <sub>3</sub>
(1232) to (0112)	J1	5° from (1232) toward (0112)	(110) GaAs // (0112) Al <sub>2</sub> O <sub>3</sub>	[011] GaAs // [2021] Al <sub>2</sub> O <sub>3</sub>
	J2	10° from (1232) toward (0112)	(110) GaAs // (0112) Al <sub>2</sub> O <sub>3</sub>	[011] GaAs // [2021] Al <sub>2</sub> O <sub>3</sub>

Along the zone between the (0001) and (11 $\bar{2}$ 0) planes of Al<sub>2</sub>O<sub>3</sub>, relatively reflective deposits of (111) GaAs were found almost parallel to the (11 $\bar{2}$ 3), (11 $\bar{2}$ 5) and (11 $\bar{2}$ 6) Al<sub>2</sub>O<sub>3</sub> planes even though the (11 $\bar{2}$ 3) and (11 $\bar{2}$ 6) are only 18.9 degrees apart; an angle of only 5 deg separates the (11 $\bar{2}$ 5) and (11 $\bar{2}$ 6) planes. These relationships were somewhat unexpected and will be investigated further. Growths on (11 $\bar{2}$ 2) and (11 $\bar{2}$ 1) Al<sub>2</sub>O<sub>3</sub> seem to be consistent with the twin relationships of (111) GaAs near (11 $\bar{2}$ 0) and (11 $\bar{2}$ 3) Al<sub>2</sub>O<sub>3</sub>.

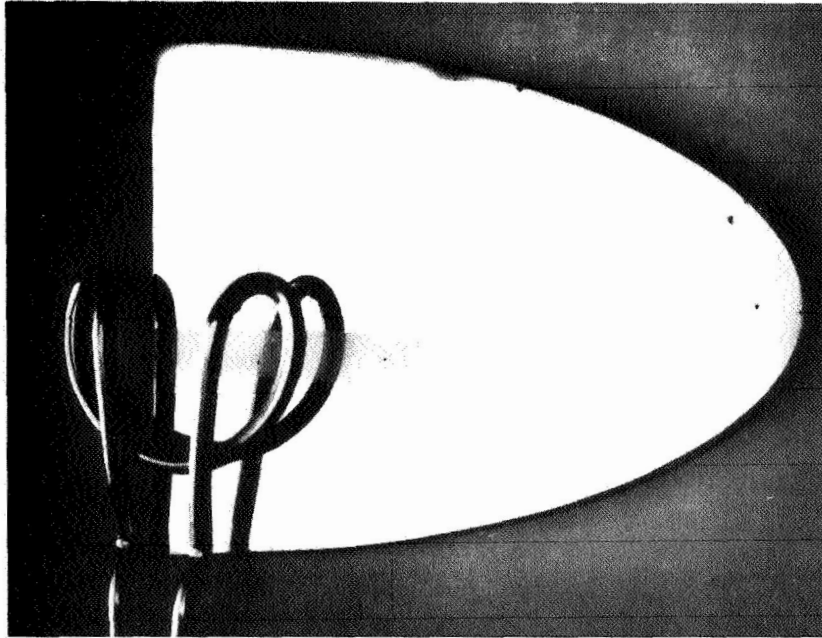
An angle of only 26 deg separates (11 $\bar{2}$ 3) Al<sub>2</sub>O<sub>3</sub> and (01 $\bar{1}$ 2) Al<sub>2</sub>O<sub>3</sub>; yet, as indicated in Table XI, three different modes of epitaxy have been seen. It is not obvious why a substrate cut 9 deg off the (01 $\bar{1}$ 2) produces (110) GaAs || (01 $\bar{1}$ 2) Al<sub>2</sub>O<sub>3</sub>, when (111) GaAs is found on (01 $\bar{1}$ 2) Al<sub>2</sub>O<sub>3</sub> if it is used as the plane of deposition. The (110) GaAs growth is consistent, however, with the results found for the J1 and J2 orientations which are on the zone between the (12 $\bar{3}$ 2) and (01 $\bar{1}$ 2) Al<sub>2</sub>O<sub>3</sub> planes. However, it is clear that additional studies are required to help explain these observations and to distinguish between matrix and twin relationships.

X-ray measurements (crystal perfection). -- X-ray rocking-curve measurements are being carried out on several of the GaAs/Al<sub>2</sub>O<sub>3</sub> samples previously established as having good electrical properties and crystal structure. Preliminary results indicate a considerable range of line broadening, with the samples that exhibit lower twin densities and higher mobilities also giving the narrowest rocking-curve widths, i. e., displaying the smallest distribution of misoriented regions about the primary orientation direction.

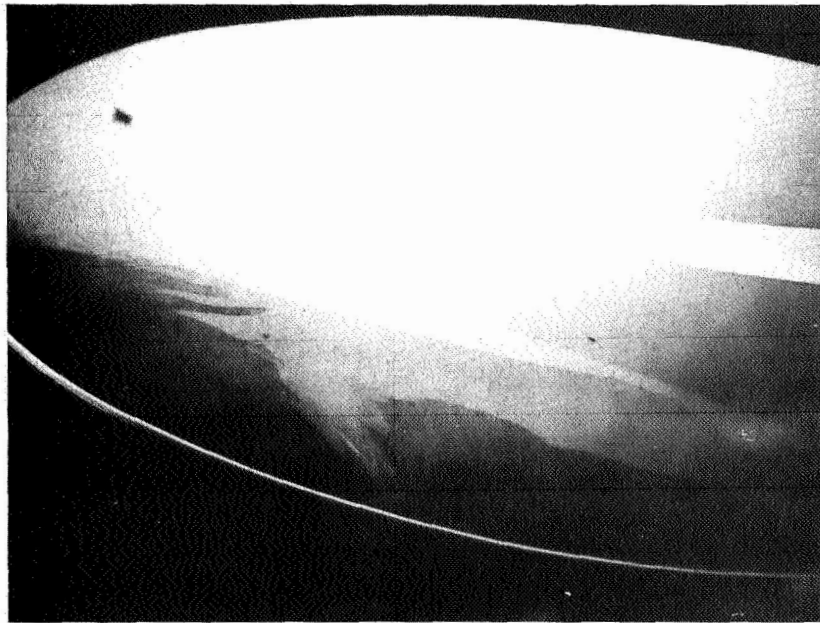
Usually no microtwins have been detected in the GaAs films grown on (0001) Al<sub>2</sub>O<sub>3</sub> when mirrorlike films are obtained. However, an unusual condition has been noted when large grains are present in the larger slices of Verneuil Al<sub>2</sub>O<sub>3</sub>. These observations are recorded in Figure 28. The film (Figure 28a) has replicated the structure in the Al<sub>2</sub>O<sub>3</sub>, as observed between crossed polaroids (Figure 28b). X-ray evaluation has shown the large grain to be about 1.5 deg off the basal plane. The poor quality film growth in this area may be related to a high degree of strain or defect structure in this grain area, formed in the crystal during its cooling from temperatures of about 2000C to room temperature, and not to misorientation; high quality films have been grown on good substrates as much as 4 deg off the (0001) plane. Lang topography will be used to evaluate this premise further.

Si on Al<sub>2</sub>O<sub>3</sub>. -- In accordance with Item 9 of the Statement of Work of Modification #1 of this contract, Autonetics has submitted during this nine-month period a total of 40 samples of epitaxial Si on Al<sub>2</sub>O<sub>3</sub>. Included have been films grown with the (111), (100), and (110) orientation with thicknesses ranging from 1400Å to 1.1μm, as requested by the Technical Monitor.

In order to prepare these films, a completely new deposition system was built in a laboratory area removed from that used for GaAs studies. This system utilizes Si deposition techniques previously developed at Autonetics. Control of the (110) Si growth would not have been feasible had not previous orientation studies been described (Ref. 6).



(a)



(b)

Figure 28. (0001)  $Al_2O_3$  (a) with GaAs Film; (b) without Film, as Seen Between Crossed Polaroids



## Substrate Surface Properties

### LEED and Auger spectroscopic analysis of $Al_2O_3$ surfaces. -- Auger spectroscopy

and LEED were used at the North American Rockwell Corporation (NR) Science Center to examine the effects of various cleaning treatments of the (0001) surface of  $\alpha-Al_2O_3$ . Stimulation for this work was provided by the observation that the quality of GaAs epitaxial growth on such surfaces is strongly dependent on surface treatment, among other factors. Two-dimensional structural changes caused by such treatments are reflected in the LEED pattern. Associated compositional changes, including impurities, should be detectable with Auger electron spectroscopy.

Two groups of samples have been examined. The first group was subjected to various cleaning treatments and annealed at high temperatures in a  $H_2$  atmosphere in the CVD reactor and then exposed to atmospheric conditions for about a week prior to insertion into the LEED system. The samples of this group were backed with 2000Å of vacuum-deposited Ta; heating in the LEED system was then accomplished by passing current through the Ta coating. To minimize atmospheric contamination, the second group of samples was not Ta backed, was placed in acetone immediately after surface treatment, and was not removed until just prior to the LEED examination.

Three substrates (a), (b) and (c), of the first group were studied. These had been subjected to the following treatments in  $H_2$ : (a) 30 min at 700C; (b) 30 min at 1200C; (c) 30 min at 1200C followed by 60 min at 900C. Because of severe atmospheric contamination, it was not possible to observe a LEED pattern from any of these specimens without in situ heating. Auger analysis revealed copious quantities of C on the surface, in addition to  $O_2$  and Al. Heating sample (a) to 725C caused some reduction in C and the appearance of a (1 x 1) LEED pattern, indicative of a bulk arrangement of surface atoms. Considerable diffuse background in the LEED pattern indicated that the surface was not well-ordered. After heating at about 900C the Auger peak due to C nearly disappeared, and a (4 x 4) LEED pattern was observed. However, in attempting to heat the sample to higher temperatures, thermal stresses caused by the heating current through the Ta deposit cracked the specimen.

Sample (b) was found to be heavily contaminated with C and cracked during an initial thermal treatment in vacuum. Sample (c) was heated indirectly by clamping it to a Ta strip and passing current through the strip. Because of poor thermal contact, however, the substrate could not be heated above about 800C. This treatment resulted in some reduction of a heavy initial deposit of C and the appearance of a diffuse (1 x 1) pattern.

Two samples of the second group were studied. One was cleaned in acetone and then heated at 1300C for 60 min; the other was processed by placing it in hot  $HF-HNO_3$  solution for 10 min. Both were stored in acetone until studied. A slightly diffuse (1 x 1) pattern was observed from both of these samples immediately after insertion into vacuum. Auger analysis revealed very little C, indicating that acetone was quite effective in preventing environmental contamination. Heating the samples to a maximum attainable temperature of about 1000C caused some improvement in the (1 x 1) pattern as well as near removal of the Auger peak due to C.

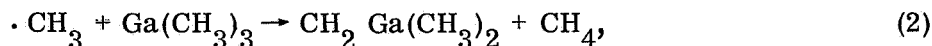
The results of these preliminary studies suggest that the surface condition as determined by LEED and Auger spectroscopy is not strongly dependent on various cleaning procedures used. Since the GaAs epitaxial studies show a definite dependence on high-temperature treatment of the surface, structural or chemical changes must occur that are not revealed by LEED and Auger spectroscopy. Alternatively it is possible that any changes caused by surface treatment are masked by the effect of exposing the sample to the atmosphere and acetone. Before proceeding further with this study, it will be necessary to make a thorough evaluation of the effect of environmental conditions on surface structure and chemistry.

### Reaction Mechanisms

The use of organo-metallics for semiconductor film formation has caused concern for the possibility of C contamination in the films. Graham (Ref. 7) has reported that the pyrolysis of TMG in an Ar carrier gas at 520C produced a metallic-looking film containing 8.0% C. Plust (Ref. 8) described the production of Ga of semiconductor purity by photolysis of triethylgallium, but Graham obtained gray-black solids containing metallic Ga using Plust's process. In both cases, a probable reaction mechanism involves free radical formation,



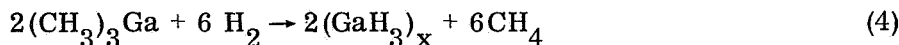
with the free radical either extracting at least one H atom from another TMG molecule,



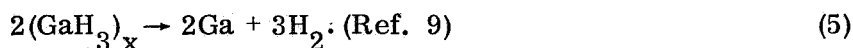
or combining with another radical to form ethane,



To minimize reaction (1) and the possible subsequent reactions involving intermediate organo-metallic compounds, H<sub>2</sub> was initially chosen as the carrier gas in order to suppress and/or tie up any free radicals that may be formed. However, it is possible that the H<sub>2</sub> could also be instrumental in generating secondary reactions such as



and



It is not known if the formation of free Ga is important to the present mechanism of growth of GaAs by the TMG-AsH<sub>3</sub> process. If it is, then one might consider, for example, a mechanism involving the following steps: (1) the formation initially of a mobile interface layer of Ga; (2) conversion of the surface layer to the Ga-V compound by reaction and/or absorption of the Group V element; and (3) rearrangement of the molecule via ionic forces to stabilize an As bond at the interface. If on the other hand the GaAs is formed exclusively away from the substrate, especially in vapor containing excess As, then molecular growth on the surface and rearrangement controlled by ionic

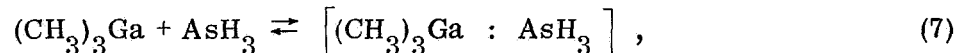
forces at the surface could also take place. For this to occur, however, one might expect the primary reaction to involve the formation of GaAs by a direct chemical reaction involving TMG and AsH<sub>3</sub>:



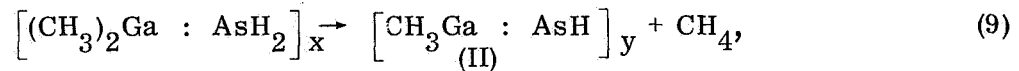
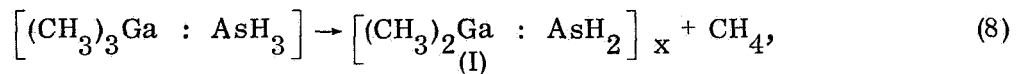
This reaction would be expected to occur equally well with an inert carrier gas. Therefore, starting with the second quarter of this program, He was investigated as a carrier gas in the CVD process.

The successful formation of GaAs from TMG and AsH<sub>3</sub> in essentially an inert atmosphere (neglecting the H<sub>2</sub> formed from the decomposition of excess AsH<sub>3</sub>) lends further evidence to the view that the primary reaction is as indicated in reaction (6) above. By keeping the AsH<sub>3</sub> in excess, pyrolysis of TMG to form nonvolatile carbonaceous-Ga products in the inert atmosphere does not take place.

Slight differences were in evidence between the H<sub>2</sub> - and He-carrier studies, in that intermediate reaction products are more clearly visible in the reactor as a volatile greenish-black powder when He is used as the carrier gas. This could be an undecomposed polymeric product formed from an unstable TMG:AsH<sub>3</sub> addition compound,



followed by stepwise release of CH<sub>4</sub>, as in (8) and/or (9),



with the formation of GaAs as the end product (reaction (6)). Compounds I and/or II in equations (8) and (9) may not be stable in a H<sub>2</sub> atmosphere.

## CONCLUSIONS

1. The trimethylgallium (TMG)-arsine (AsH<sub>3</sub>) process for growing GaAs has been shown to be capable of producing epitaxial films (on single-crystal insulating substrates such as Al<sub>2</sub>O<sub>3</sub> and MgAl<sub>2</sub>O<sub>4</sub>) with essentially bulk electrical properties in the carrier concentration range of ~ 10<sup>16</sup> to 10<sup>17</sup> cm<sup>-3</sup>.
2. The carrier concentrations of the films are found to depend primarily on the purity of the starting materials and carrier gases used in growing the films.
3. The quality of the GaAs film is also dependent on the relative AsH<sub>3</sub>-TMG concentrations, which can be changed to control the conductivity type, carrier concentration, and resistivity of the film.
4. Reflection electron diffraction studies indicate that some improvement in the crystal structure of thin layers can be achieved by appropriate annealing procedures.

5. GaAs/ $Al_2O_3$  orientation-relationship studies have, to date, indicated (0001)  $Al_2O_3$  to be the best plane for growth of (111) GaAs.

6. Diethylzinc (DEZ) is effective as a p-type dopant for the GaAs films. The final hole concentration is dependent on the growth rate and temperature of deposition as well as the dopant concentration.

7. The TMG-AsH<sub>3</sub> process can be used to produce high quality films on bulk GaAs, with mobility limitations appearing to be dependent specifically on the purity of the starting materials.

## REFERENCES

1. Tietjen, J. J., and Amick, J. A., *J. Elect. Soc.* 113, 724 (1966).
2. Knight, J. R., Effer, D., and Evans, P. R., *Solid State Electron.* 8, 178 (1965).
3. Zanowick, R. L., *J. Elect. Soc.* 114, 146C (1967).
4. Manasevit, H. M., and Simpson, W. I., *J. Elect. Soc.* 115, 66C (1968).
5. Manasevit, H. M., *Appl. Phys. Letters* 12, 156 (1968).
6. Manasevit, H. M., Nolder, R. L., and Moudy, L. A., *Trans. TMS-AIME* 242, 465 (1968).
7. Graham, W. A., and Gatti, A. R., A. D. Little, Inc., Cambridge, Mass.,  
Final Report, Contract AF19(604)-4975, 31 Dec. 1960.
8. Plust, H. G., U. S. 2,898,278; August 4, 1959.
9. Greenwood, N. N., and Wallbridge, M., *J. Chem. Soc.*, 3912, (1963).

## APPENDIX A. NEW TECHNOLOGY

### An Alternate Process for Preparing GaAs by the TMG-AsH<sub>3</sub> Reaction

The substitution of an inert carrier gas, namely He, for H<sub>2</sub> in the TMG-AsH<sub>3</sub> process for GaAs deposition has provided GaAs films with mobilities equivalent to and in some cases greater than those films formed to date in a H<sub>2</sub> atmosphere. The higher perfection may possibly be related to the nonreducing atmosphere provided by He and to the consequent absence of certain impurities which might, when H<sub>2</sub> is used, be incorporated into the film by reduction reactions. These effects are recorded on pages 9, 15 through 18, 21, and 22.